Diss. ETH No. 6861

INFLUENCE OF SUPERCONDUCTIVITY AND MAGNETISM ON TRANSPORT PROPERTIES OF RARE EARTH RHODIUM BORIDE COMPOUNDS

A dissertation submitted to the
SWISS FEDERAL INSTITUTE OF TECHNOLOGY ZURICH

for the degree of
Doctor of Natural Sciences

presented by
WALTER ODONI
Dipl. Phys. ETH
born on the 9th April 1950
citizen of Hochdorf (Luzern)

accepted on the recommendation of
Prof. Dr. J.L. Olsen, referee
Dr. H.R. Ott, co-referee
Prof. Dr. B.S. Chandrasekhar, co-referee

ADAG Administration & Druck AG

Zürich 1981

für Yvonne

CONTENTS

1 INTRODUCTION

The rare earth rhodium borides have only been known since 1977, neverthe-
less they attracted a widespread interest in the short period since then.
The reason for the special attention is the broad variety of magnetic and
superconducting properties of these compounds which stimulated the research
on the old question of coexistence of long range magnetic order and super-
conductivity (Ginsburg 1956). In the past this problem was studied in
systems like $La_{1-x}Gd_x$ (Hein, Falge, Matthias and Corenzwit 1959) but all
these systems had the disadvantage of inhomogeneous distribution of the
magnetic ions in the sample (for a review see Roth 1977). In the rare earth
rhodium borides the magnetic ions form a regular lattice. Therefore the
problem of inhomogenity is avoided but the problem of single phased samples
remains.

For a discussion of superconductivity and magnetism it is essential
to measure real bulk properties. A small amount of an impurity phase which
becomes or remains superconducting,profoundly affects the electrical con-
ductivity whereas the measurements of the thermal conductivity probes
genuine bulk properties.

When a material transforms from the normal to the superconducting state
conduction electrons condense in a ground state with no entropy and con-
sequently they do not contribute to the thermal conduction. The electronic
thermal conductivity in the superconducting phase will be reduced. Phonons
are no more scattered at the condensed electrons, therefore the lattice
contribution to the thermal conductivity is enhanced. Thus measurements
of the thermal conductivity give information on superconductivity.

When a material undergoes a magnetic phase transition it changes from a disordered to a magnetically ordered state. This transition also influences the mean free path of the electrons and with this the electrical resistance and the thermal conductivity. Therefore, measurements of the electrical resistivity and the thermal conductivity provide complementary information on superconductivity and magnetism.

In this thesis we discuss the thermal conductivity and the electrical resistivity of four rare earth rhodium borides, namely $LuRh_4B_4$, $HoRh_4B_4$, $ErRh_4B_4$ and $SmRh_4B_4$, each of them showing different behaviour.

$LuRh_4B_4$ shows superconductivity, $HoRh_4B_4$ exhibits ferromagnetic order. A study of these two compounds gave us the "background information" for the compounds where both phenomena occur.

$ErRh_4B_4$ becomes superconducting at 8.7 K (Matthias, Corenzwit, Vandenberg and Barz 1977) and returns to a normal magnetically ordered state at $\sim$ 0.9 K (Fertig, Johnston, DeLong, McCallum, Maple and Matthias 1977). Of special interest is the temperature range between 1.2 and 0.87 K where magnetic order sets in but the electrical resistivity still remains zero (Moncton, McWhan, Eckert, Shirane and Thomlinson 1977). With thermal conductivity measurements we hope to gain more information about the order parameter in this temperature range.

$SmRh_4B_4$ shows superconductivity below 2.68 K down to at least 50 mK. A lambda-type anomaly in the specific heat indicates a magnetic phase transition at $\sim$ 0.8 K without destruction of superconductivity. The interaction of the normal electrons with the localized magnetic Sm^{3+} ions cannot be seen in the electrical resistivity because of the superconduc-

tivity but according to the theory of thermal conductivity in the super-conductor containing magnetic impurities by Ambegaokar and Griffin (1964) this interaction should affect the thermal conductivity due to a pair-breaking effect of the Cooperpairs by localized magnetic moments. The thermal conductivity therefore provides a tool to study this pairbreaking effect.

2. EXPERIMENTAL METHODS

The results reported in this thesis were taken in either a ^{3}He-^{4}He dilution refrigerator or in a conventional ^{4}He pumping cryostat. A longitudinal or a transverse magnetic field could be applied on the sample space. The longitudinal field was provided by a small supercon-ducting selenoid for fields up to 8 kOe. A circular bent head supercon-ducting coil (Harris 1934) was used to produce a transverse magnetic field with a maximum strength of 5 kOe. The rather complicated form of a circular bent head coil instead of a pair of rectangular coils was chosen in order to improve the homogeneity over a typical sample length. The optimised parameters, taking into account the small space for a coil in our refrigerator, were finally chosen so that the homogeneity of the magnetic field over 2 cm was better than 1%.

2.1 ^{3}HE-^{4}HE DILUTION REFRIGERATOR

The ^{3}He-^{4}He dilution refrigerator used in this work is self con-structed and covers the temperature range from 35 mK to 4 K. This tech-nique of cooling substantially below 0.3 K has the advantage, in compari-son to other known methods, that it works continually. An excellent de-scription of this technique is found in Lounasmaa's book "Experimental Principles and Methods Below 1 K" (1974) or in papers by Wheatley, Vilches and Able (1968) or Wheatley, Rapp and Johnson (1971).

As can be seen from figure 2.1 our design is conventional. There is a single continuous heat exchanger. To prevent the superfluid He
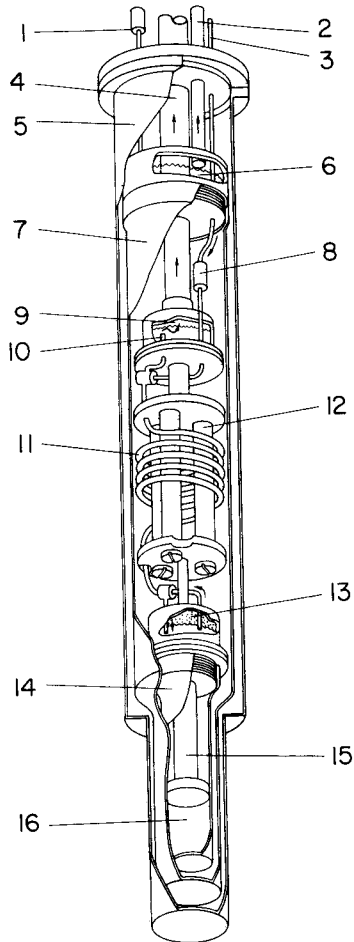
<u>Figure 2.1</u>

1 Impedance for continous filling of the 1 K plate; 2 pumping tube for 1 K plate; 3 ^{3}He condensing line; 4 still pumping line; 5 vacuum chamber; 6 1 K plate; 7 heat shield; 8 flow impedance; 9 still; 10 inlet of ^{4}He rich mixture; 11 continous heat exchanger; 12 graphite support; 13 mixing chamber; 14 heat shield; 15 sample holder; 16 experiment.

film flow through the pumping tube in the still, we used an idea of
Wheatley et al (1971) by pumping the still through a heated tube whereby
the film on the outside of the tube is evaporated. With this construction
one improves the ^{3}He/^{4}He ratio and reduces the danger of thermal con-
duction shorts between still and 1 K plate. The surface of the bottom in
the mixing chamber was increased by cutting thin grooves into the copper
bottom to improve the thermal contact to the outside. A copper extension
is connected to the mixing chamber and reaches into the tail of the vacuum
chamber around which the magnet is fixed. There are two heat shields sur-
rounding the sample. The inner shield is fixed at the mixing chamber and
mainly prevents residual ^{4}He exchange gas from reaching the sample. The
radiation shields are made out of copper coil foils i.e. of tighly packed
insulated thin parallel copper wires which are reinforced by a thin layer
of epoxy (Anderson, Salinger and Wheatley 1961). The advantage of such a
foil is the good heat conduction in one direction and the suppression of
eddy currents perpendicular to the direction of heat conduction.

Six carbon resistor thermometers(see below) are mounted at strategical
points of the dilution unit to monitor the cooling. Heaters in the still,
on the mixing chamber and on the sample holder served to establish the
desired temperatures. All heaters are supplied by a dc current taken from
a battery to avoid any ripple. An electronic feedback system (SHE tempera-
ture controller) allowed us to stabilise the sample holder on a fixed
temperature within 0.0005 K. The performance of the whole cryostat de-
pended strongly on the correct ^{3}He-^{4}He mixture. With the optimised mix-
ture we reached an ultimate temperature of 35 mK. The cooling power in the
low temperature region is then a function of the still heater power which

defines the ^{3}He circulation rate. Figure 2.2 shows the temperature de-
pendent cooling power with the still heater power as a parameter.

The appropriate temperature region for the use of a dilution refri-
gerator is below 1 K. Measurements above 1 K often suffered of instabili-
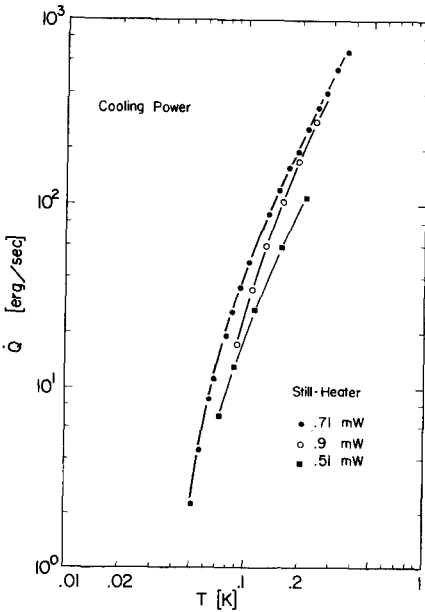ties of the temperature.

Figure 2.2
Cooling power of the dilution
refrigerator as a function of
the heat imput in the still.

2.2 ^{4}HE CRYOSTAT

To extend the temperature region beyond the easily accessible range of a
dilution refrigerator we designed a ^{4}He cryostat suitable for thermal and
electrical conductivity measurements up to 50 K. The design is shown in

figure 2.3. A radiation shield surrounds the sample and is thermally anchored to a copper block. The copper block together with the radiation shield and sample can be screwed to a brass flange which is in direct contact with the ^{4}He bath. According to the number of turns the copper block is screwed into the flange, the thermal contact to the ^{4}He bath can be varied.
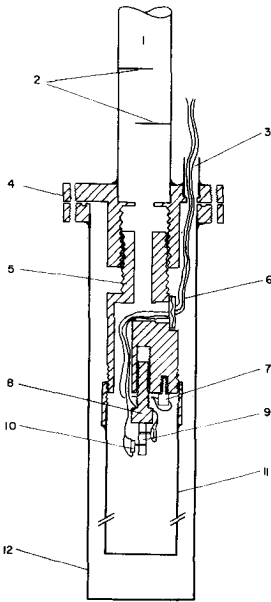
Figure 2.3
^{4}He cryostat: 1 pumping tube; 2 ra-
diation shields; 3 seal for leads;
4 vacuum flange; 5 copper block;
6 plug; 7 carbon glass resistor; 8
sample holder; 9 sample; 10 thermo-
meter; 11 radiation shield; 12 vacuum
chamber.

2.3 THERMAL AND ELECTRICAL CONDUCTIVITY MEASUREMENTS

For the thermal conductivity measurement we used the method of a steady heat flow through the sample (c.f. fig. 2.4). In this case, a known rate of heat $\dot{Q}$ is supplied at one end of the sample and removed at

Experimental arrangement

Figure 2.4

1 Sample holder; 2 thermally anchored leads; 3 copper camps; 4 thermometer 2;
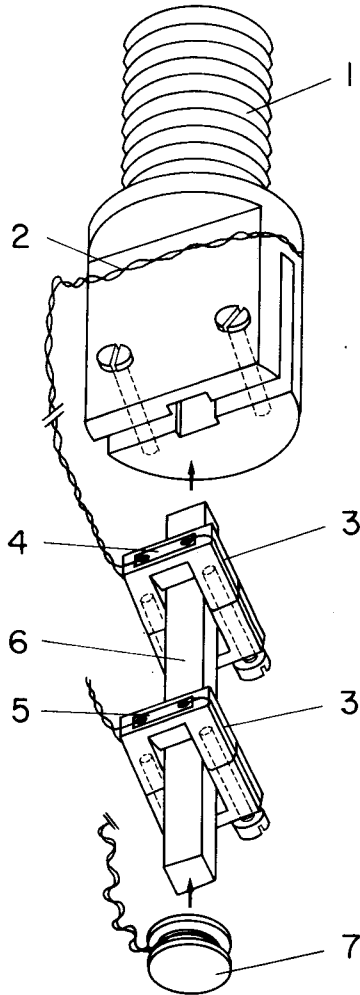5 thermometer 1; 6 sample; 7 Sample heater.

the other end. Two thermometers separated by a distance L on the sample
determine the temperature difference ΔT between them. The thermal conduc-
tivity is then given by the relation

$$\lambda(\bar{T}) = \frac{L}{F} \frac{1}{\Delta T} \dot{Q} \qquad (2.1)$$

where F is the (uniform) cross section of the sample. Assuming ΔT is
small compared to the mean temperature $\bar{T}$ of the thermometers this value
of the thermal conductivity λ corresponds to the temperature $\bar{T}$. In our
measurements ΔT was normally ∿2-3% of the mean temperature and never ex-
ceeded 7%. Only thermometer 1 was calibrated. The resistances of the two
thermometers were first measured in the absence of a heat current. Then
with a heat current present, the temperature of the sample holder was re-
gulated to give the same reading of thermometer 2 as before. The two values
of thermometer 1 then defined ΔT and $\bar{T}$. This procedure reduced the error
in ΔT by using only one resistance versus temperature fit.

2.4 THERMOMETRY

For the calibration of the sample thermometers we used a CMN thermometer
in connection with a calibrated germanium resistor. The experimental
arrangement is shown in figure 2.5. Powdered CMN sits in one of two ba-
lanced pick-up coils. Thermal contact to the sample holder is provided
through a coil foil slab which is pressed into a copper block. A super-
conducting primary coil produces an alternating field of 87 Hz and maxi-
mal amplitude of 0.7 Oe. The primary can be moved relatively to the pick-
up coils so as to balance the signals coming from the two secondaries.
The difference of the induced pick-up coil signals is proportional to the

susceptibility of the CMN and therefore inversely proportional to the temperature. The CMN thermometer was calibrated against a Ge thermometer (Lake Shore model no. GR-200A-50, calibrated between 0.3 and 1.4 K). The superconducting critical temperature T_c of Ir served as a check point for the reliability of the calibration. We estimate our absolut temperature error below 1 K to about 2%. For higher temperatures a carbon glass resistor was used (Lake Shore model CGR-1-500, calibration range 1.4-80 K).
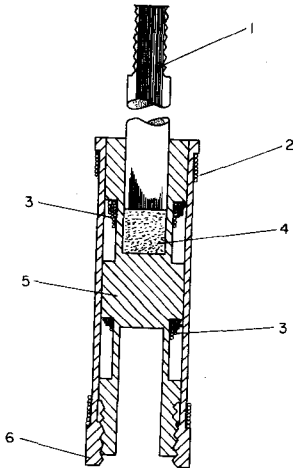
Figure 2.5

CMN thermometer: 1 coil foil slab; 2 primary coil; 3 pick-up coil; 4 CMN; 5 epoxy block; 6 screw for balancing.

The sample thermometers were made out of Allen Bradley carbon resistors for the high temperature range or of Matsushita resistors for the temperature below 1 K. They were carefully ground down to slices of approximate 0.2 mm thickness. This reduces the heat capacity, improves the thermal contact and makes it possible to glue them to the flat surface of copper clamps which were pressed onto the sample. The calibration points were fitted to a polynomial in logR (Clement and Quinell 1952). The whole temperature range was divided into several overlapping fit regions with different coefficients.

3. THEORETICAL BACKGROUND

The thermal conductivity is defined by

$$h_i = - \lambda_{ij} \frac{\delta T}{\delta x_j} \qquad (3.1)$$

where the h_i's are the components of a vector $\vec{h}$. $\vec{h}$ is the heat flow

across unit cross section perpendicular to $\vec{h}$, T is the temperature and

the λ_{ij} are the components of a second rank tensor of the thermal conduc-

tivity. For an isotropic solid or a crystal with cubic symmetry this

equation reduces to the simpler form

$$\vec{h} = - \lambda \text{grad } T. \qquad (3.2)$$

The heat current therefore can be described in these materials by a

single value λ which is temperature and material dependent.

In the following sections we give a short description of the main

mechanisms which determine λ in the temperature range of our measurements.

3.1 THERMAL CONDUCTION BY PHONONS

The heat current $\vec{h}$ due to phonons can be written as (Berman 1976)

$$\vec{h} = \sum N(\vec{q}) \ \hbar\omega(\vec{q}) \ \vec{v}_g(\vec{q}) \qquad (3.3)$$

where $N(\vec{q})$ is the phonon density, $\vec{q}$ the wave vector, $\hbar\omega$ the energy of a

phonon with frequency ω and $\vec{v}_g(\vec{q})$ the group velocity of propagation. The

sum includes all phonon modes. In the relaxation time approach of the

thermal conductivity and with the simplifying assumption of the Debye

model of specific heat (Kittel 1971) (3.3) yields

$$\lambda_g = \frac{k_B}{2\pi^2 v_g} \left(\frac{k_B}{\hbar}\right)^3 T^3 \int_0^{\Theta/T} \tau(x) \frac{x^4 e^x}{(e^x-1)^2} \, dx \qquad (3.4)$$

for the lattice thermal conductivity λ_g where $x = \dfrac{\hbar\omega}{k_B T}$, Θ = Debye temperature and $\tau(x)$ = effective relaxation time for a phonon with energy $\hbar\omega$.

Equation (3.4) can be generalised by adding different scattering rates τ_i^{-1} to a total scattering rate $\tau_{tot}^{-1}(x)$ (Klemens 1951)

$$\tau_{tot}^{-1}(x) = \sum_i \tau_i^{-1}(x). \qquad (3.5)$$

The mean free path $l(x)$ of the heat carriers is related to the relaxation time $\tau(x)$ by

$$l(x) = v(x) \, \tau(x). \qquad (3.6)$$

The problem of calculating λ_g is to find the appropriate relaxation rate for different scattering mechanisms.

At the lowest temperatures the phonons are mainly scattered by crystal boundaries including internal grain boundaries. In this case the scattering is independent of frequency (see e.g. Berman 1976) and given by $\tau_b^{-1} = v/k$ where k is the mean free path of the phonons due to boundary scattering and typically of grainsize of the crystal. Using (3.4) this yields a T^3 dependence of the thermal conductivity:

$$\lambda_{g_{boundary}} = 7.2 \frac{k_B k}{2\pi^2 v^2} \left(\frac{k_B}{\hbar}\right)^3 T^3. \qquad (3.7)$$

At higher temperatures, depending on the actual mean free path k, scattering by electrons will become predominant. The relaxation rate τ_{ge}^{-1} of this process, assuming a spherical Fermi surface, is proportional to ω (see e.g. Klemens 1956) and, if phonon-electron scattering is the only scattering mechanism one gets

$$\lambda_{ge} = \frac{T^2}{A} \tag{3.8}$$

again using (3.4). A is a constant, given by inserting τ_{ge} into (3.4).

Still higher temperatures will make the impurities and finally the umklapp processes of importance (see e.g. Olsen and Rosenberg 1953). We do not consider this scattering here because our temperature range is too limited to see these interactions.

3.2 THERMAL CONDUCTION BY ELECTRONS

The main contribution to the thermal conductivity in a metal is normally given by the electrons and we can write the total thermal conductivity λ_{tot} by

$$\lambda_{tot} = \lambda_g + \lambda_e \tag{3.9}$$

where λ_g is the lattice part of the thermal conductivity and λ_e the electronic contribution.

In a discussion of the electronic thermal conductivity λ_e one follows similar lines of reasoning as in section 3.1. The important scattering mechanisms at intermediate and low temperatures are the electron-phonon and the electron-defect scattering described by relaxation times τ_{eg} and τ_{ed} respectively. If one assumes Matthiessen's rule (1862), that is the

additivity of the thermal resistivities, the electronic part of the thermal conductivity λ_e may be written

$$\lambda_e^{-1} = \frac{\beta}{T} + \alpha T^2 \qquad (3.10)$$

at low temperature (Ziman 1960). The first term on the right side is related to the defect and impurity scattering and is connected with the residual resistivity ρ_o through

$$\beta = \frac{\rho_o}{L_o} \qquad (3.11)$$

with the Lorenz number $L_o = 24.5 \ nWatt\Omega/K^2$. The second term describes the scattering of electrons by phonons.

3.3 THERMAL CONDUCTION IN A SUPERCONDUCTOR

The thermal conduction in a superconductor is governed by the same processes as in the normal metal. Due to the rearrangement of the density of states of the electrons $N(E)$ in the superconducting state and the development of a temperature dependent energy gap $\Delta(T)$ these processes are different in strength in the superconductor compared to the normal metal. The occurrence of a gap reduces the number of excitations which are responsible for the thermal conduction of the electrons. Therefore the electronic part of the thermal conductivity is reduced. The lattice part on the other hand is increased on account of the reduced phonon-electron scattering. Below about $t = 0.2$, t being the reduced temperature T/T_c, the thermal conductivity is comparable to an insulator.

The temperature variation in the superconducting state depends strongly
on the specific dominant scattering mechanisms at T_c and the relative
amount of electronic and lattice contributions to the thermal conductivity
as was demonstrated in measurements of Olsen (1952) on lead and lead -
bismuth alloys.

The first quantitative description of the behaviour of the electronic
and lattice thermal conductivity in the superconducting state on the basis
of the BCS theory of superconductivity (Bardeen, Cooper and Schrieffer
1957) was given by Geilikman and Kresin (1958) and Geilikman (1958). Their
calculations were restricted to the case where the impurity scattering of
the electrons is dominant and the phonon-electron scattering is the limi-
ting process for the lattice thermal conductivity. In the same year
Bardeen, Rickayzen and Tewordt (1958) published a theory on the thermal
conductivity of superconductors. We refer to it as the BRT-theory. They
deal with the electronic contributions when the dominant scatterers are
impurities or phonons. BRT also calculated the effect of the electrons
on the lattice conductivity. Although BRT cannot explain the strong de-
pression of the thermal conductivity in the case of lead (Olsen 1952)
where electron-phonon scattering is dominant theyexplain the other mecha-
nisms quite well (Sousa 1969).

For a dominant electron-defect scattering BRT give an equation for
the electronic thermal conductivity in the superconducting state λ_e^s

$$\lambda_e^s = - \frac{2N(E_F)v_o l}{3T} \int_{\Delta(T)}^{\infty} dE \; E^2 \; \frac{\delta f}{\delta E} \; . \tag{3.12}$$

f is the Fermi function $f = (e^{E/k_B T} + 1)^{-1}$, v_o the electron velocity on the

Fermi surface and l the mean free path of the electrons. Wyder (1965)
showed that the mean free paths in the normal and superconducting state
are the same. E is the excitation energy of the BCS quasiparticles, that
is

$$E = (\varepsilon^2 + \Delta^2)^{1/2} \tag{3.13}$$

where ε is the energy of the normal electrons measured from the Fermi sur-
face and $2\Delta(T)$ is the superconducting energy gap. For $\Delta(T) \equiv 0$ (3.12)
describes the normal state electronic conductivity. The ratio of the two
electronic conductivities λ_e^s in the superconducting state and λ_e^n in the
normal state can be written as

$$\frac{\lambda_e^s}{\lambda_e^n} = \frac{2F_1(-y) + 2y\ln(1 - e^{-y}) + y^2(1 + e^y)^{-1}}{2F_1(0)} \tag{3.14}$$

with $y = \Delta(T)/k_B T$ and

$$F_1(-y) = \int_0^\infty z(1 - e^{(z+y)})^{-1} dz. \tag{3.15}$$

$F(-y)$ is tabulated by Rhodes (1950). A more convenient form for the cal-
culation of (3.14) is given by Geilikman (1958)

$$\frac{\lambda_e^s}{\lambda_e^n} = \frac{6}{\pi^2} \frac{\Delta(T)^2}{k_B T} \left[\exp(\Delta(T)/k_B T) + 1 \right]^{-1} + 2k_B T \sum_{s=1}^{\infty} (-1)^{s+1} \exp(-s\Delta(T)/k_B T)$$

$$x \frac{1}{s^2} + 2\Delta(T) \ln\left[1 + \exp(-\Delta(T)/k_B T) \right]. \tag{3.16}$$

$\Delta(T)$ was calculated by Mühlschlegel (1959) for $1 > t > 0.2$.

We evaluated (3.16) nummerically and show the results in figure 3.1.
Although the ratio $2\Delta(0)/k_B T_c$ in the BCS theory for weak coupling supercon-
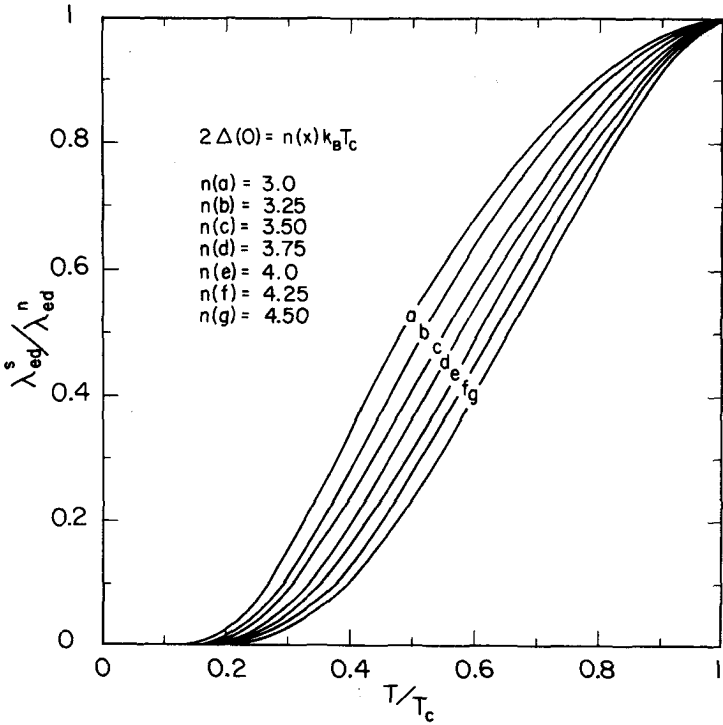
Figure 3.1

Ratio of the electronic thermal conductivity in the superconducting state λ_e^s to the electronic thermal conductivity in the normal state λ_e^n if impurity and defect scattering is dominant.

ductor is 3.53, this ratio may be different in a real superconductor. We included therefore values for $2\Delta(0)/k_B T_c$ between 3.0 and 4.5.

If not only impurity scattering but also electron-phonon processes are important Kadanoff and Martin (1961) deduced a formula for the ratio λ_e^s/λ_e^n as a function of a single parameter a which gives the ratio of the

phonon resistance to the impurity resistance at the critical temperature
T_c. λ_e^s/λ_e^n is then given by

$$\frac{\lambda_e^s}{\lambda_e^n} = \frac{3}{2\pi^2}\int_0^\infty d(\epsilon\gamma)(\gamma\epsilon)^2 \mathrm{sech}^2\left[\frac{1}{2}\left\{\epsilon^2+(\gamma\Delta)^2\right\}\right]^{1/2}\left[1 + a(T/T_c)^3\left[\frac{\gamma\epsilon}{\left\{(\gamma\epsilon)^2+(\gamma\Delta)^2\right\}^{1/2}} + a(T/T_c)^3\right]^{-1}\right.$$

(3.17)

with $\gamma = 1/k_B T$ and a taken from (3.10)

$$a = \frac{\alpha T_c^3}{\beta}.$$

(3.18)

For $a = 0$ (impurity scattering dominant) (3.17) is equivalent to (3.14).

BRT also discussed the lattice thermal conductivity in a super-
conductor. Assuming that the phonons are scattered only by electrons
BRT give a formula for the lattice thermal conductivity λ_g^s in the super-
conducting state

$$\lambda_g^s = D(T/\Theta)^2 \int_0^\infty \frac{x^3 dx}{(e^x-1)(1-e^{-x})g(x)}$$

(3.19)

where D is a constant independent of temperature, Θ the Debye temperature
and $g(x)$ the ultrasonic attenuation coefficient in the superconducting
state (for longitudinal phonon modes) normalized to the attenuation coeffi-
cient in the normal state:

$$g(x) = \frac{\alpha_s}{\alpha_n} = \frac{l_s^{-1}}{l_n^{-1}} = \frac{\tau_n^{-1}}{\tau_s^{-1}}$$

(3.20)

α is the attenuation coefficient, the indices n and s refer to the normal
and superconducting state. $g(x)$ can be written as

$$g(x) = \frac{1-e^x}{x} (2J_1 + J_2) \qquad (3.22)$$

with

$$J_1(x) = \int_{\Delta(T)}^{\infty} dE \left[\frac{\varepsilon^2 + E x k_B T}{\varepsilon \varepsilon'} \right] f(E) f(-E') \qquad (3.23)$$

and

$$J_2(x) = \int_{\Delta(T)-xk_B T}^{-\Delta(T)} dE \left| \frac{EE'}{\varepsilon \varepsilon'} \right| \left[1 - \frac{\Delta^2}{\varepsilon \varepsilon'} \right] f(E) f(-E') \qquad (3.24)$$

where $E' = E + xk_B T$. The second integral is nonzero only if $x > 2\Delta(T)/k_B T$. This corresponds to the creation of a pair of quasiparticles which is only possible when the phonon energy is higher than the energy gap.

Because no tabulated values of (3.23) and (3.24) were available we integrated J_1 and J_2 nummerically. The singular points in the integral are eliminated by appropriate substitutions following the procedure given by Bobetic (1964). The results are shown in figure 3.2 for various reduced temperatures t as a function of x. t is calculated assuming the BCS value $2\Delta(0)/k_B T_c = 3.53$.

The ratio λ_g^s/λ_g^n describing the relative increase of the lattice thermal conductivity in the phonon-electron scattering regime is shown in figure 3.3 for different values of $2\Delta(0)/k_B T_c$. Nummerical values of this ratio can be found in a paper by Lindefeld and Rohrer (1965) as a function of $\Delta(T)/k_B T$.

The enormous enhancement of the lattice thermal conductivity in the superconducting state is damped down at low temperatures by different
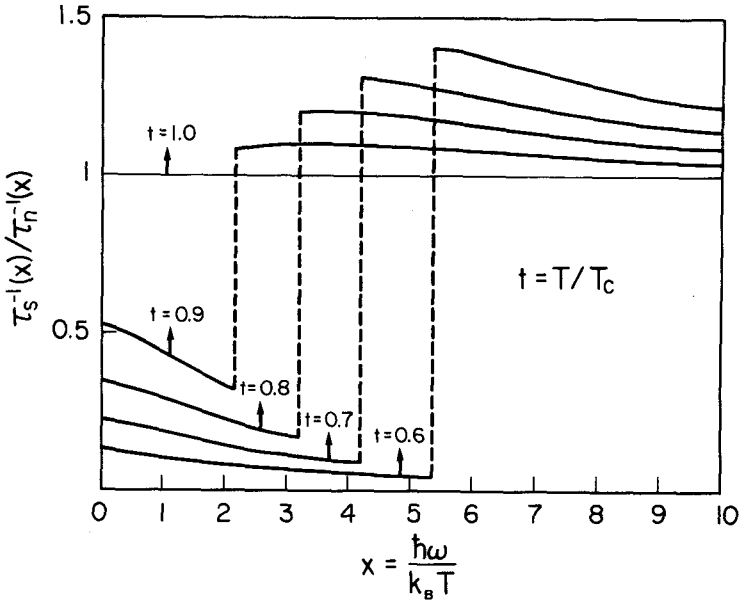
Figure 3.2

Ratio of the relaxation rates due to phonon-electron scattering in the superconducting state to that in the normal state as a function of the frequency.

scattering mechanisms. As Klemens and Tewordt (1964) pointed out, point defect scattering can have a pronounced effect on the lattice thermal conductivity in the superconducting state because the phonon-electron scattering is highly reduced. They took this into account by adding to the BRT equation an additional point defect scattering term with $\tau \propto \omega^4$.
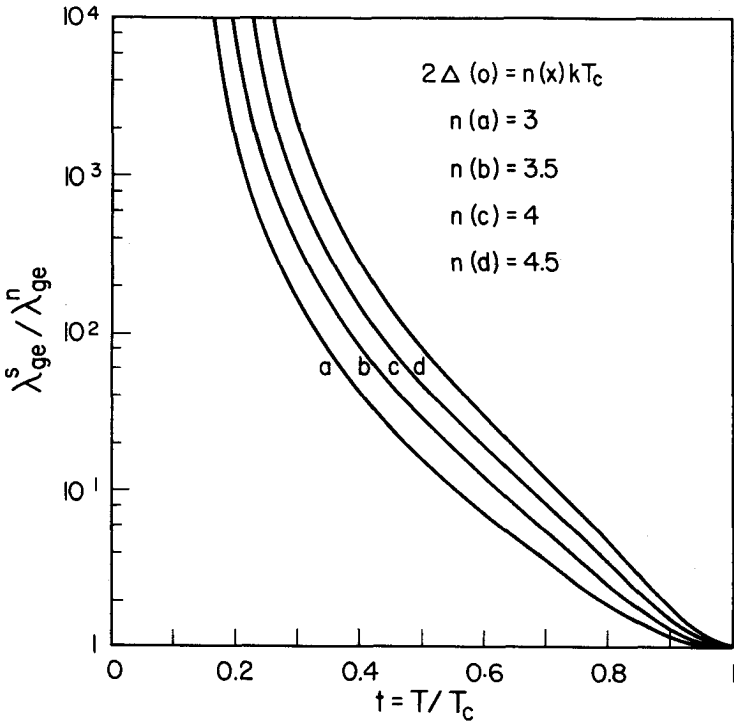
Figure 3.3

Ratio of the lattice thermal conductivity in the superconducting state to that in the normal state if electron scattering is dominant.

At the lowest temperatures the boundary scattering term takes over and we expect a T^3 dependence of the lattice thermal conductivity.

4. INFLUENCE OF SUPERCONDUCTIVITY AND MAGNETISM ON TRANSPORT PROPERTIES
OF RARE EARTH RHODIUM BORIDE COMPOUNDS

In 1977 Matthias, Corenzwit, Vandenberg and Barz presented a new system
of rare earth ternary compounds. This system with the formula $RERh_4B_4$ where
RE stands for rare earth exhibits either superconductivity or magnetic
ordering or both phenomena. A survey of the magnetic T_m as well as the su-
perconducting transition temperatures T_c is presented in figure 4.1. In
addition we included a third temperature T_λ where a lambda-type anomaly
in the specific heat is observed that points to a phase transition at low
temperature.

The compounds with RE = Gd, Tb, Dy and Ho were originally found to
order ferromagnetically whereas for RE = Nd, Sm, Er, Tm and Lu supercon-
ductivity was found (Matthias et al 1977). The compound $ErRh_4B_4$ was later
found to exhibit reentrant superconductivity, wherein ferromagnetic
ordering of the Er^{3+} magnetic moments around T_m destroys superconductivity
(Fertig, Johnston, DeLong, McCallum and Maple 1977). The isostructural
compounds with Nd (Hamaker, Woolf, MacKay, Fisk and Maple 1979) and Sm
(Hamaker, Woolf, MacKay, Fisk and Maple 1979) revealed in further investi-
gations the possible coexistence of long-range magnetic order and super-
conductivity. This broad variety of superconductivity and magnetism in a
system with a regular sublattice of magnetic ions stimulated an extensive
study on the interaction of superconductivity and magnetism.

Since electrical resistivity measurements sometimes simulate super-
conductivity even with only a small fraction of a superconducting phase

in a sample, we have chosen thermal conductivity measurements as a probe
for the bulk properties of these compounds.

In the following sections we present electrical and thermal conduc-
tivity measurements of four different members of the group of $RERh_4B_4$
compounds each of them showing quite different behaviour. Starting with
$LuRh_4B_4$ as a representative of a superconductor with no magnetic inter-
ference we proceed to the other extreme to $HoRh_4B_4$ which only orders
magnetically. $ErRh_4B_4$ shows both phenomena but in an exclusive way where-
as in $SmRh_4B_4$ there is strong evidence for the coexistence of supercon-
ductivity and magnetic order.

4.1 SAMPLES

All the samples were made available by Profs. B.T. Matthias and M.B. Maple
and their groups at the UCSD, La Jolla. A description of sample preparation
is found e.g. in the thesis of L.D. Woolf (1980). The structure is shown
in figure 4.2. To clarify the regular sublattice of the RE ions the inter-
atomic distances are not drawn to scale. This structure was found by Vanden-
berg and Matthias in 1977. The unit cell is primitive tetragonal and con-
tains two formula units with a pronounced clustering of Rh and B atoms.
As the above authors pointed out, this clustering behaviour is a general
feature of some high transition temperature superconductors.
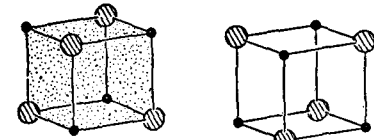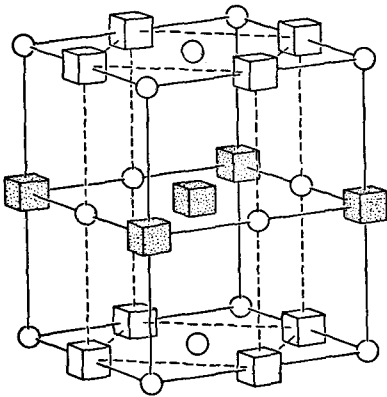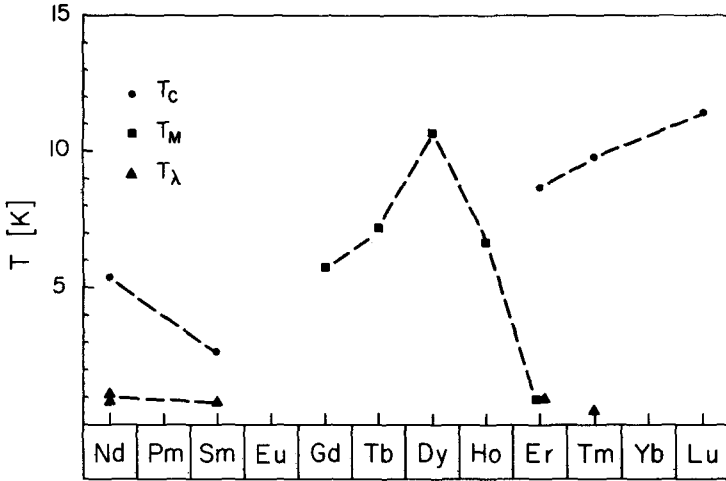
RERh$_4$B$_4$

○ RE   ◍ Rh   • B

Figure 4.1

Survey of ferromagnetic T$_m$ and superconducting T$_c$ *critical tem-peratures of* RERh$_4$B$_4$; T$_\lambda$ indicates a lambda-type anomaly in the specific heat. In Tm, the specific heat is not measured through the whole anomaly.

Figure 4.2

Crystal structure of RERh$_4$B$_4$ compounds. Dashed lines indicate the tetragonal unit cell. For clarity the cubes representing Rh$_4$B$_4$ clusters are not drawn to scale (MacKay 1979).

4.2 INFLUENCE OF SUPERCONDUCTIVITY ON THERMAL CONDUCTIVITY: $LURh_4B_4$

The nonmagnetic $LuRh_4B_4$ shows only superconductivity. This enables us to study the effect of superconductivity on the thermal conductivity in this series without any interference with magnetic ordering. $LuRh_4B_4$ becomes superconducting at 11.45K. Specific heat measurements by Woolf, Johnston, McKay, McCallum and Maple (1979) as well as magnetisation measurements by Ott, Cambell, Rudigier, Hamaker and Maple (1981) indicate that $LuRh_4B_4$ is a type II superconductor. The lattice specific heat data revealed a complicated phonon spectrum which could be explained by assuming a molecular crystal model with Lu and Rh_4B_4 clusters as a "diatomic" crystal (Woolf et al 1979). Below about 15 K an extended Debye model of the specific heat can fit the data equally well. The Debye temperature of this fit turns out to be $\Theta_D = 444$ K which is in reasonable agreement with sound velocity measurements of Schneider, Levy, Johnston and Matthias (1980) who found for the sound velocity of longitudinal waves $v_s = 6$ km/s.

The thermal conductivity data of $LuRh_4B_4$ in the range of 2 to 25 K are given in figure 4.3. Also shown in this graph is the thermal conductivity in an applied magnetic field parallel to the heat current $\dot{Q}$. From electrical resistivity measurements T_c is found to be 9.5 K in our sample. Unfortunately it was not possible in our apparatus to restore the normal state below 9 K. The thermal conductivity above the critical temperature T_c cannot be described by a linear temperature dependence. Below T_c we observe a substantial increase above the roughly extrapolated values of the normal state. These two features are typical for metals in which the normal state conductivity of the electrons is not governed completely by

impurity scattering. A similar behaviour is found e.g. in a lead-bismuth alloy with 0.5% bismuth (Olsen 1952). Additionally, the lattice thermal conductivity must be considerable.

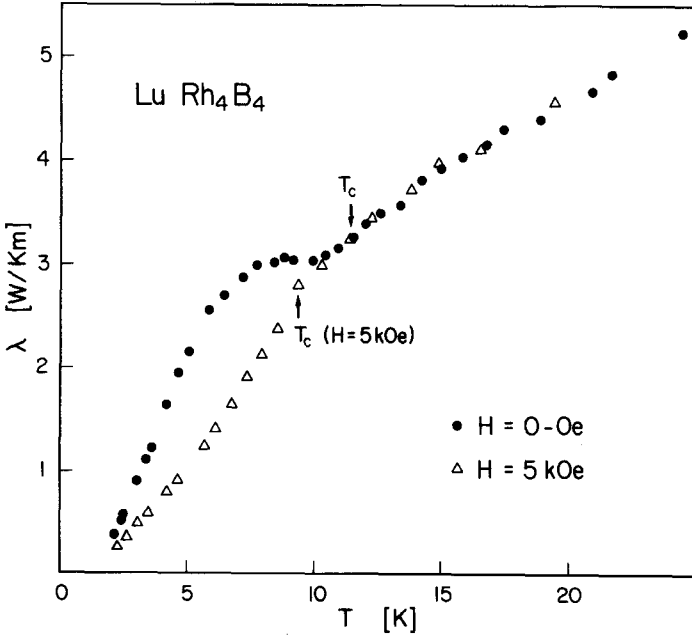Figure 4.3

Thermal conductivity of LuRh$_4$B$_4$ in zero magnetic field and in an applied field of 5 kOe parallel to the heat current.

In order to analyse our data we separate the total thermal conductivity in a lattice and an electronic part (c.f. (3.9)). For the electronic thermal conductivity in the normal state λ_e^n we use the additive resistance approximation (c.f. (3.10) and (3.11))

$$\lambda_e^n = \frac{T}{\alpha T^3 + \rho_o/L_o} \tag{4.1}$$

The residual resistivity ρ_o of our sample is 9.9×10^{-8} Ωcm, the residual
resistivity ratio RRR = 16.4. The resistance starts to deviate from ρ_o
around 13 K due to electron-phonon interactions, therefore we have to allow
for a small value of α which is related to the same interactions. The
electron-phonon scattering is responsible for the downward curvature of
λ_e^n with increasing temperature. For the lattice part we use (3.4). Con-
sidering the scattering mechanisms which are important in the supercon-
ducting state and may have some influence on the normale state lattice con-
ductivity, we write the overall relaxation rate $(\tau_g^n)^{-1}$ of the normal state
as a sum of a boundary, a phonon-electron and a phonon-impurity rate.
(3.4) can then be written as (Gupta and Wolf 1972)

$$\lambda_g^n = \frac{k_B}{2\pi v^2} \left[\frac{k_B}{h} \right]^3 T^3 \int_o^{\Theta/T} \frac{x^4 e^x dx}{(e^x-1)^2 (1/k + CTx + GT^4x^4)} \, . \tag{4.2}$$

k is the boundary mean free path. C and G are related to the phonon mean
free path due to the conduction electrons and point defects. In the super-
conducting state, only the phonon-electron scattering rate will be changed,
λ_g^s is thus given by

$$\lambda_g^s = \frac{k_B}{2\pi v^2} \left[\frac{k_B}{h} \right]^3 T^3 \int_o^{\Theta/T} \frac{x^4 e^x dx}{(e^x-1)^2 (1/k + CTxg(x) + GT^4x^4)} \tag{4.3}$$

Below $t = 0.2$ according to the BRT theory (c.f. fig. 3.1) the electronic
thermal conductivity can be ignored and the lattice thermal conductivity
is mainly limited by boundary scattering. λ_g^s/T^3 therefore should be a

constant. The lowest points of the thermal conductivity λ^s indeed tend to a T^3 dependence. Taking this value we can write for the low temperature thermal conductivity $\lambda^s_g = \lambda^s$ for $t < 0.2$

$$\lambda^s = 4 \times 10^{-2} T^3 \ \frac{W}{K^4 m} \tag{4.4}$$

The mean free path k in the integral (4.3) is therefore given by

$$k^{-1} = 650 \ \frac{k_B}{2\pi v^2} \left(\frac{k_B}{h}\right)^3 \tag{4.5}$$

We introduced (4.5) into (4.4) and used ρ_o/L_o in (4.1). The energy gap relation $2\Delta(0)/k_B T_c = 4.1$ was taken from the specific heat measurements by Woolf et al (1979). There was no combination of the remaining parameters which reproduced the experimental results over the whole temperature range. The energy gap relation therefore was used as an additional unknown parameter. The best fit to our data is shown in figure 4.4. The parameters used for this fit are

$$2\Delta(0)/k_B T_c = 3.5$$
$$\alpha = 2.5 \times 10^{-4} \ m/KWatt$$
$$\beta = 4.05 \ mK^2/Watt$$
$$(Yk)^{-1} = 650 \ K^4 m/Watt$$
$$G/Y = 3.9 \times 10^{-3} \ m/Watt \tag{4.6}$$

with

$$Y = \frac{k_B^4}{2\pi^2 h^3 v^2}$$

The electron-phonon scattering term described by α is small compared to the electron-defect scatteringterm β. The use of the BRT theory for pure electron-defect scattering is therefore justified.
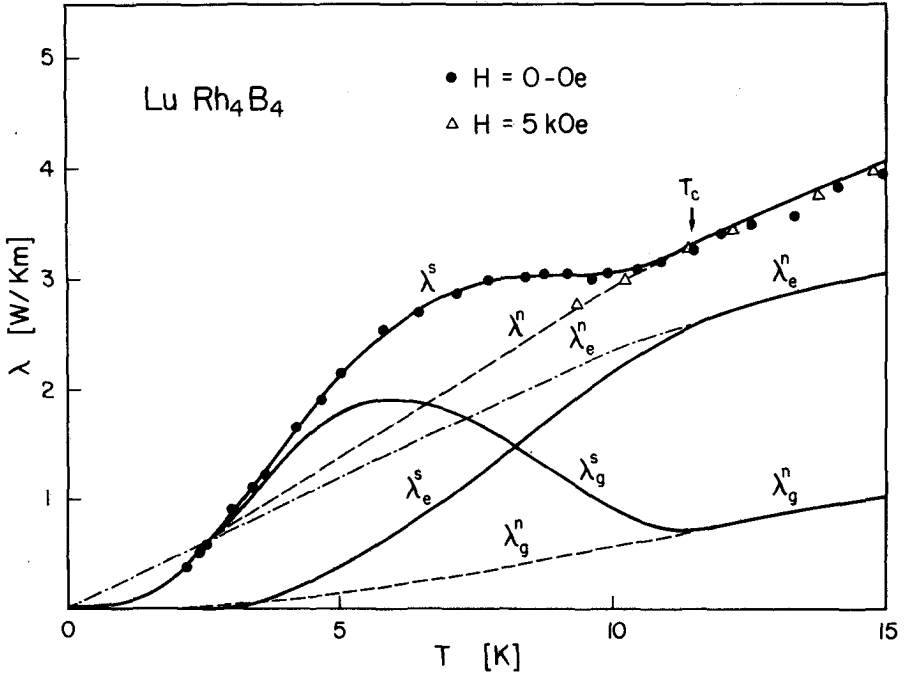
Figure 4.4

Thermal conductivity of $LuRh_4B_4$ with calculated lattice and electronic contribution. Lower indices e and g refer to electronic and lattice contribution, upper indices n and s to normal and superconducting state respectively (Odoni, Keller, Ott, Hamaker, Johnston and Maple 1981).

At $T_c = 11.45$ K the lattice part of the thermal conductivity λ_g^n is about 23% of the total thermal conductivity. Below T_c λ_g^s increases rapidly but the increase is reduced due to the point defect scattering. Below about 4 K the thermal conductivity is mainly limited by boundary scattering of the phonons.

In the Debye approximation of specific heat a Debye temperature of 444 K corresponds to a velocity of sound of 3.4 km/s (assuming 8.7×10^{28} atoms/m^3). With (4.5) we deduce a phonon mean free path in the supercon-ducting state due to boundary scattering of about 10 µ. There exist no grain size measurements of our sample which can confirm this estimate.

4.3 FERROMAGNETISM IN A RARE EARTH RHODIUM COMPOUND: $HoRh_4B_4$

$HoRh_4B_4$ whose low temperature physical properties have recently been in-
vestigated in some details (Ott, Woolf, Maple and Johnston 1980; Maple
Hamaker, Johnston, McKay and Woolf 1978) orders ferromagnetically at
T_m = 6.7 K (Matthias et al 1977) due to a spontaneous alignment of the
localized 4f electron magnetic moments of the Ho^{3+} ions. Ott, Keller,
Odoni, Woolf, Maple, Johnston and Mook (1981) showed that the magnetic
contribution to the specific heat, zero field magnetisation, electrical
resistivity and thermal expansion measurements can be described very
accurately by using mean field theory and assuming an effective spin = $1/2$.
We do not repeat the details of this discussion. The aim of this section
is to show qualitatively the influence of the magnetic ordering on electri-
cal conductivity and thermal conductivity. We hope to find some features
in these transport properties which are characteristic for magnetic ordering
and may give a hint on magnetic ordering in other ternary compounds of
this type where the situation is not at all so clear (see e.g. $SmRh_4B_4$).

We measured the electrical resistivity ρ of our sample in the tempera-
ture range between 1.5 K and 15 K with a low frequency four probe technique.
Assuming Matthiessen's rule of the additivity of the different resistive
processes (for a review of deviations of Matthiessen's rule see e.g. J.
Bass 1972) we can write the total resistivity $\rho(T)$ at any temperature as
(Taylor and Darby 1972)

$$\rho(T) = \rho_{res} + \rho_{ph}(T) + \rho_m(T) \qquad (4.7)$$

where ρ_{res} is the residual resistivity which is independent of tempera-
ture and depends only on crystalline imperfections and impurities in the
sample. The scattering of conduction electrons by phonons leads to a
temperature dependent resistivity $\rho_{ph}(T)$. The third term $\rho_m(T)$ finally is
due to the magnetic contribution caused by the disorder of the spin system.
Experimentally it is often difficult to separate   the different tempe-
rature dependent terms but in the case of HoRh$_4$B$_4$ this is easier because
the magnetic contribution ρ_m is not masked by the phonon term.

Figure 4.5 shows the electrical resistivity of HoRh$_4$B$_4$ between 1.5 K
and 10 K. The resistivity ρ is constant below 2.5 K with the value ρ_{res}
and also between T_m and 10 K. Hence, the temperature dependence of ρ below
10 K is due only to a magnetic scattering term $\rho_m(T)$ which is constant in
the paramagnetic state and tends to a constant value well below T_m. One
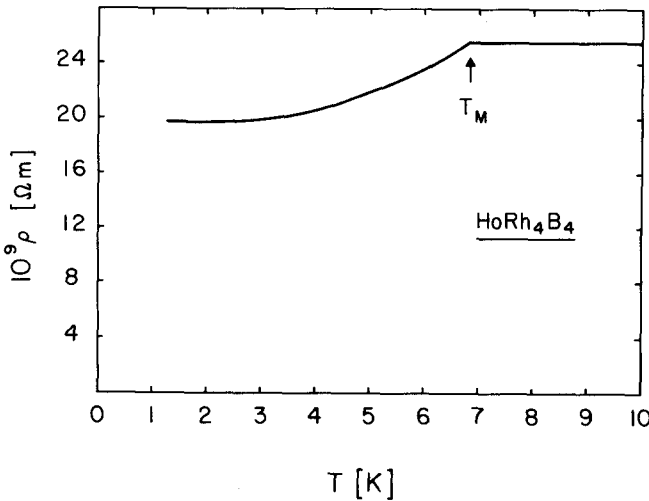can show (Ott et al 1981) that the temperature dependent term below T_m is

Figure 4.5
Electrical resistivity of HoRh$_4$B$_4$. T_M indicates the magnetic ordering
temperature.

proportional to $1 - (M/M_o)^2$ where M is the magnetisation at the temperature T and M_o the magnetisation at T = 0.

Figure 4.6 shows the thermal conductivity of the same sample in the temperature range of 100 mK up to 12 K. As may be seen, the data above and well below T_m depend linearly on temperature. The steepening in the slope of the thermal conductivity versus temperature below the ordering temperature T_m is interpreted as an increase of the mean free path of the electrons due to the reduced scattering on magnetic moments and is consistent with the behaviour of the reduced electrical resistivity. There is too much scattering in these data to detect a sharp edge at T_m as found in the electrical resistivity.
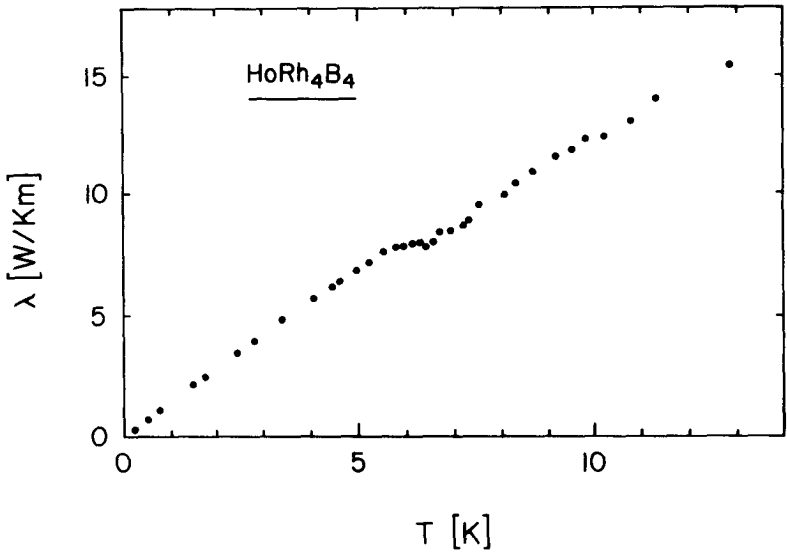

Figure 4.6

Thermal conductivity of $HoRh_4B_4$.

4.4 REENTRANT SUPERCONDUCTIVITY: $ErRh_4B_4$

Among the $RERh_4B_4$ compounds, $ErRh_4B_4$ is probably the best known member

because of its peculiar superconducting and magnetic properties. $ErRh_4B_4$

shows a superconducting transition at $T_{c1} = 8.9$ K on zero external magnetic

field (Matthias et al 1977). At a second lower temperature $T_{c2} \sim 0.9$ K

the electrical resistivity appears again (Fertig et al 1977). Suscepti-

bility and specific heat measurements indicated that around T_{c2} a long range

magnetic order appears. Neutron scattering experiments have confirmed ferro-

magnetic order below T_{c2} with a considerable precursor scattering starting

at about 1.2 K (Moncton, McWhan, Eckert, Shirane and Thomlinson 1977).

These data showed an ordered magnetic moment of 5.6 μ_B per Er^{3+} ion in the

ferromagnetic phase consistent with the value of $\sim$ 6 μ_B from magnetisation

measurements. This value is well below the Hund's rule value of 9.59 μ_B

per Er^{3+} ion. Ott, Fertig, Johnston, Maple and Matthias (1978) suggested

that crystalline electric fields lift the degeneracy of the Er^{3+} Hund's

rule ground state.

The ac electrical resistance and the susceptibility showed a thermal

hysteresis in a range of about 50 mK around T_{c2} in disagreement with the

first neutron scattering experiments. Similar hysteretic behaviour is found

in the thermal conductivity measurements by Odoni and Ott (1979). Sub-

sequently, hysteresis was found in the neutron scattering as well (Moncton,

McWhan, Schmidt, Shirane, Thomlinson, Maple, MacKay, Woolf, Fisk and Johnston

1980).

The specific heat near T_{c2} (Woolf, Johnston, MacKay, McCallum and

Maple 1979) shows a rather unusual behaviour. A broad specific heat maxi-

mum is found around 1 K. Superimposed on it is a lambda-type anomaly with
a width of about 70 mK which peaks at a temperature $T = 0.93$ K. In addition
to this special feature around T_{c2} the calorimetric study provided strong
evidence for the partially lifted degeneracy of the Hund's rule ground
state by the crystalline electric field as proposed by Ott et al (1978).
The precursor scattering together with the specific heat anomaly and the
electrical resistivity measurements lead to the speculation that there
exists a limited region where long range magnetic order and superconducti-
vity coexist. In a discussion of these problems it is essential to know
more about real bulk properties in order to confirm that the observed effects
are not just spurious.

In the following sections we discuss thermal conductivity measurements
on $ErRh_4B_4$ in a temperature range between 0.05 K and 50 K and in an exter-
nal magnetic field up to 3 kOe with the field direction parallel or per-
pendicular to the heat flow. Our sample was a prism of polycrystalline ma-
terial with dimension of $7x1.5x1.5$ mm^3 and in previous work it was denoted
as sample A (see Ott et al 1978).

The thermal conductivity of $ErRh_4B_4$ in zero applied field is shown in
figure 4.7. There are four clearly distinguishable regions. The thermal con-
ductivity above T_{c1} is mainly due to electronic conduction. The deviation
from a nearly linear temperature dependence at higher temperature is due to
the increasing importance of electron-phonon scattering. Between T_{c1} and
~ 1.2 K the thermal conductivity behaves as in a superconductor with a small
contribution from the lattice thermal conduction. Between 1.2 K and ~ 0.9K
the thermal conductivity increases again and reaches a local maximum around
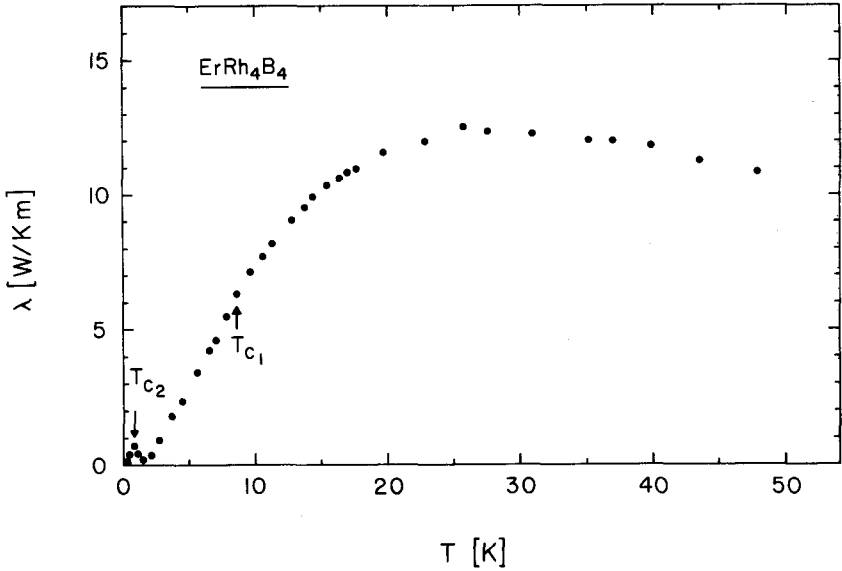0.9 K. In this temperature range we observe a thermal hysteresis of about

Figure 4.7

Thermal conductivity of $ErRh_4B_4$ in zero applied field in the temperature range of 50 mK to 50 K.

60 mK (see below). Below 0.87 K the thermal conductivity shows a linear temperature dependence as one expects for a normal metal with almost exclusive electronic conduction. In figure 4.8 we give the thermal conductivity data together with the variation due to an applied external field parallel to the heat current $\dot{Q}$. Figure 4.9 demonstrates the effect of a parallel and a perpendicular external magnetic field around 1 K. In the parallel case we expect that a magnetic field in a type II superconductor induces normal cores and reduces the average order parameter. The thermal conductivity is increased. In the perpendicular field the normal cores are much more effective in scattering the normal electrons, therefore the in-
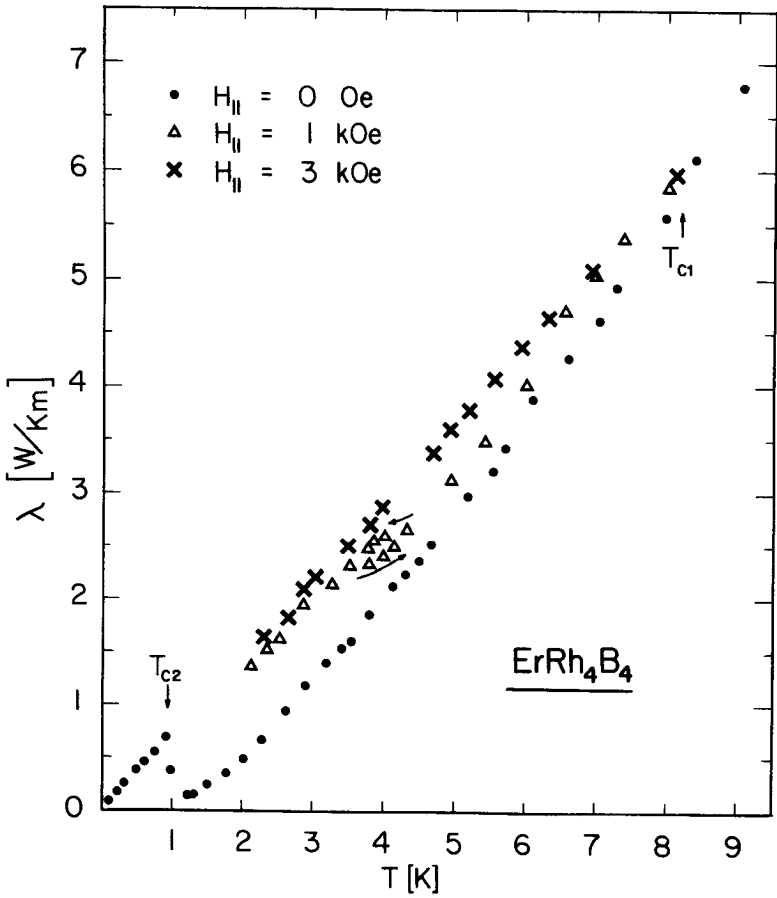
Figure 4.8

Thermal conductivity of $ErRh_4B_4$ for different applied magnetic fields parallel to the heat current.
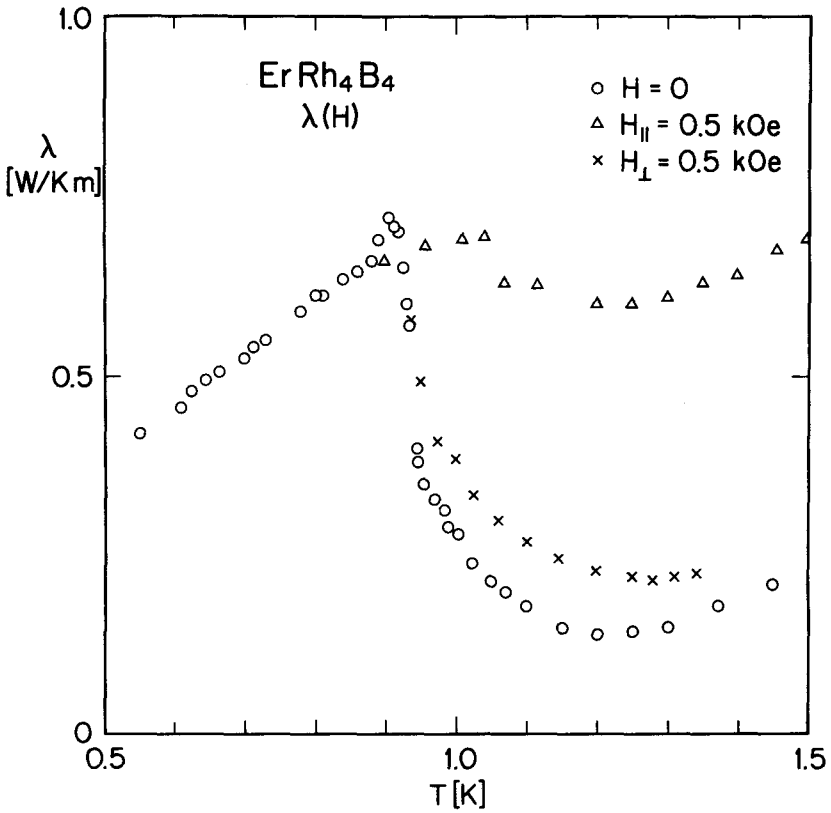
Figure 4.9

Thermal conductivity of $ErRh_4B_4$ around 1 K in an applied magnetic field of 0.5 kOe parallel and perpendicular to the heat current $\dot{Q}$ (Ott and Odoni 1980).

crease of the thermal conductivity at a given field is less pronounced
(Ott and Odoni 1980).Figure 4.10 demonstrates the hysteretic behaviour
around T_{c2}.

In comparing the thermal conductivity with the electrical resistance
of a similar sample of $ErRh_4B_4$ investigated by Ott et al (1978) (c.f. fig.
4.11) we find some equivalent features but there are several differences.
The electrical resistance at T_{c2} shows a narrow although hysteretic tran-
sition from the superconducting to the normal state. In contrast to this,
the thermal conductivity slowly increases towards lower temperatures over
a temperature region of $\sim$ 0.5 K. The value of the electrical resistance
below T_{c2} in zero external magnetic field is about 85 % of the normal state
value to which it saturates in fields greater than 2 kOe. No such satura-
tion is found in the thermal conductivity. The thermal conductivity between
T_{c1} and T_{c2} saturates to a linear temperature dependent value in a field of
3 kOe whereas one uses 12 kOe to suppress any reduction in the electrical
resistance. This difference in the two transport properties suggests that
a small amount of a second phase is present in the sample which remains
superconducting at temperatures below T_{c2} in zero external magnetic field.
These superconducting phases are too small to affect the thermal conducti-
vity but may be extended enough to electrically shorten parts of the sample.
We interprete the slow increase of the thermal conductivity below 1.2 K as
a reduction of the superconducting order parameter due to the onset of
magnetic ordering. In this temperature range superconductivity is still pre-
sent as can be seen from the electrical resistance measurements.

In analysing our data between T_{c1} and 50 K we separate the total thermal
conductivity into a lattice and an electronic contribution using (3.9),
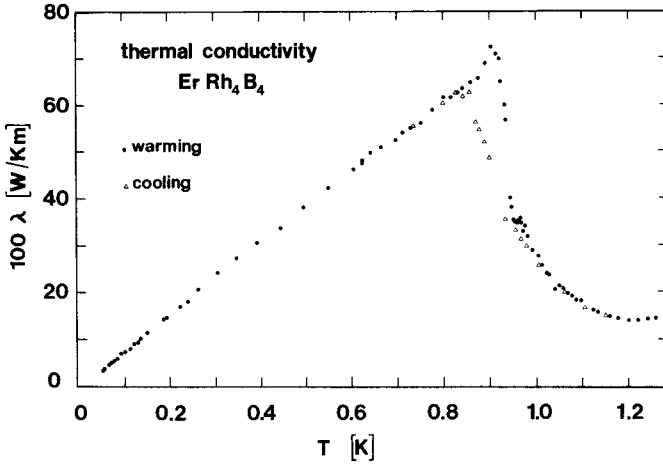
Figure 4.10

Influence of the phase transition from the superconducting (T > 1 K) to the magnetically ordered normal state (T < 1 K) on the thermal conductivity of ErRh$_4$B$_4$. Full dots denote values when warming up, open circles denote values when cooling (Odoni and Ott 1979).
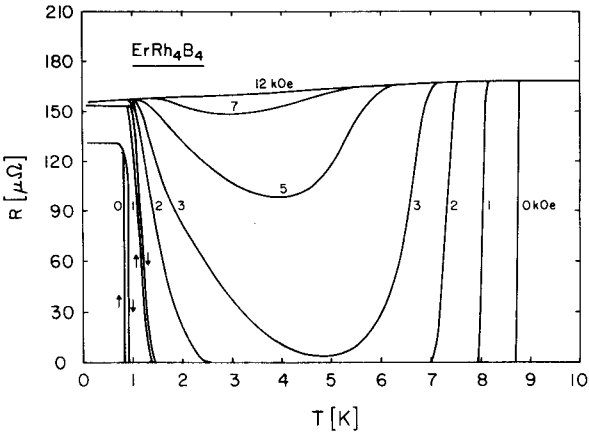
Figure 4.11

The ac electrical resistance versus temperature for a rod-shaped specimen of ErRh$_4$B$_4$ in various applied magnetic fields between 0 and 12 kOe (from Ott, Fertig, Johnston, Maple and Matthias 1978).

(3.10) and (3.11)

$$\lambda = \frac{T}{\alpha T^3 + \rho_o/L_o} + \frac{T^2}{A} \qquad (4.8)$$

To verify the assumption that the electronic contribution to the thermal conductivity is given by the ratio of the residual resistivity ρ_o and the Lorenz number L_o when electron-impurity scattering is considered, we check this relation below T_{c2} where the lattice contribution can be neglected. The residual resistivity of our sample is 3.35×10^{-8} Ωm. According to Ott et al (1978) the saturation value below T_{c2} is $\sim 95\%$ of the value above $T_{c1}$. Using the same reduction in our sample, we have a residual resistivity of 3.2×10^{-8} Ωm below T_{c2}. Together with the Lorenz number L_o, L_o/ρ_o yields 0.77 Watt/K^2m. The measured value λ/T is 0.76 Watt/K^2m and therefore justifies the above mentioned procedure. We used the following parameters to fit the thermal conductivity above T_{c1} up to 50 K:

$$\alpha = 5.6 \times 10^{-5} \text{m}/(\text{Watt K})$$
$$\beta = \rho_o'/L_o = 1.37 \ (\text{mK}^2)/\text{Watt} \qquad (4.9)$$
$$A = 500 \ (\text{K}^3\text{m})/\text{Watt.}$$

ρ_o' is the constant resistivity above T_{c1}. Figure 4.12 shows the fit with these parameters.

In analysing the behaviour of the thermal conductivity in the superconducting state, we first have to discuss the influence of the magnetic Er^{3+} ions on the superconducting properties. The depression of the superconducting critical temperature T_c in presence of impurities with localized magnetic moments is treated by Abrikosov and Gor'kov (1960). They consider the additonal scattering of the conduction electrons due to the exchange interaction. This theory is limited to systems with non-interacting magnetic
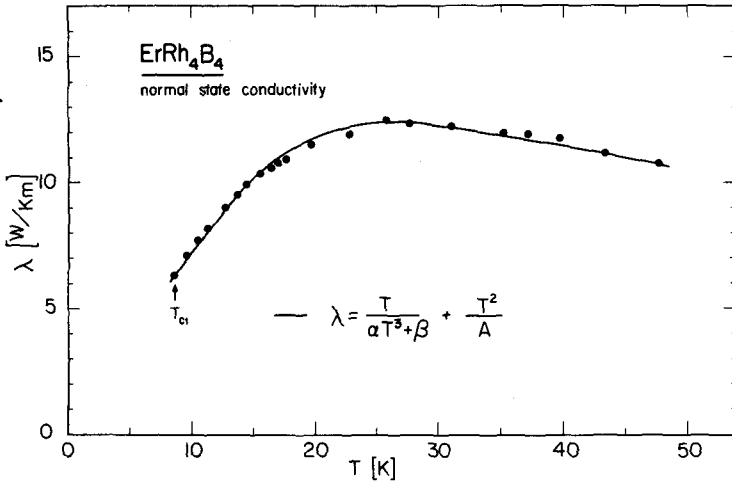
Figure 4.12

Theoretical fit to the normal state thermal conductivity of $ErRh_4B_4$. The fit includes electron-impurity and electron-phonon scattering for the electrons and phonon-electron scattering for the phonons.
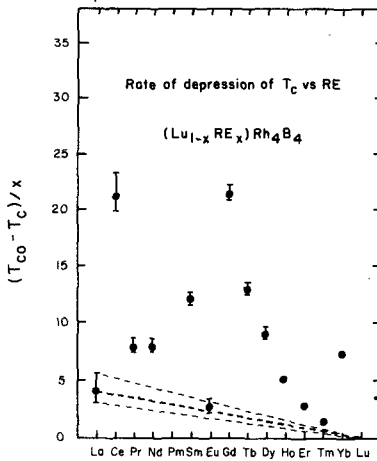

Figure 4.13

Rate of depression of T_c vs RE in $(Lu_{1-x}RE_x)Rh_4B_4$. The dashed lines are the limits of the assumed depression due to nonmagnetic effects of the substitution of Lu (MacKay, Woolf, Maple and Johnston 1980).

moments. The depression of T_c by adding to the superconductor localized

magnetic moments with a concentration n_i can be described by a universal

function n_i/n_{cri}. n_{cri} is the critical concentration where the supercon-

ductivity is totally suppressed. In an attempt to distinguish between the

magnetic and the nonmagnetic influence of a RE on T_c of these compounds,

MacKay, Woolf, Maple and Johnston (1980) measured the T_c of compounds of

the form $Lu_{1-x}RE_xRh_4B_4$. The results are shown in figure 4.13. Because the

depression rate for the nonmagnetic RE = La should be zero according to the

Abrikosov-Gor'kov theory, a straightline has been drawn to display the

assumed nonmagnetic effect of the substitution of Lu. For $ErRh_4B_4$ the de-

pression due to nonmagnetic effects is about 1.5 K, a "nonmagnetic" $ErRh_4B_4$

compound therefore would have a T_c of 9.9 K. The actual T_c is 8.7 K. This

corresponds to a ratio T_c/T_{cp} = 0.88 where T_{cp} is the superconducting cri-

tical temperature without magnetic interactions and T_c the superconducting

critical temperature in the presence of magnetic moments. Using the tabulated

values of the Abrikosov-Gor'kov function (Ramos and Sanchez 1974) this re-

duction of the critical temperature would be caused by an impurity concen-

tration n_i/n_{cri} = 0.17.

In the framework of the Abrikosov-Gor'kov theory, Ambegaokar and Griffin

(1964) calculated the ratio of the normal electronic thermal conductivity

to the electronic thermal conductivity in the superconducting state in terms

of the parameter n_i/n_{cri}. For n_i/n_{cri} = 0.17 they find an increase at t = 0.6

of λ_e^s/λ_e^n of 3% above the BRT value which is within the errorbars of our

measurements. We have therefore analysed the thermal conductivity data of

$ErRh_4B_4$ neglecting the (small) magnetic influence of the Er^{3+} ions.

The BRT theory gives an equation for the increase of the lattice ther-

mal conductivity due to the reduced probability of phonon-electron scattering

in the superconducting state. Clearly this increase is damped at low tempera-
tures by other scattering mechanisms. At the lowest temperatures the domi-
nant scattering mechanism for phonons is boundary scattering, leading to
a constant mean free path which is characterized by a T^3 dependence. Indeed
between 1.4 K and 2 K we find such a T^3 dependence as can be seen from fi-
gure 4.14. We extracted the parameter which describes the phonon-boundary
scattering and applied then the BRT theory using the parameters given in
(4.9). The result of our fit is shown in figure 4.15 where we used for $2\Delta(0)/$
$k_B T_c$ a value of 3.5. Below 1.4 K the measured thermal conductivity starts
to increase again and deviates from the theoretical curve. At this tempera-
ture magnetic ordering sets in. With the onset of long range magnetic order,
the assumption of non-interacting magnetic moments breaks down. Fisher(1979)
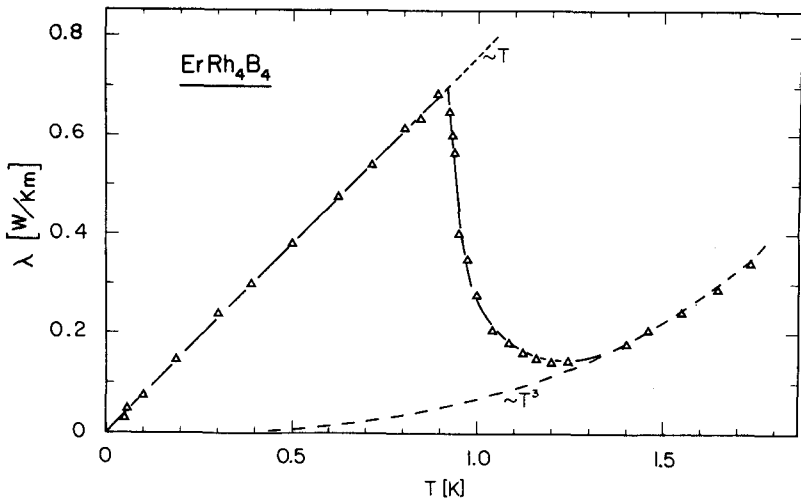
Figure 4.14
T^3 dependence of the thermal conductivity of $ErRh_4B_4$ in the temperature
range of 1.2 K to 1.9 K.
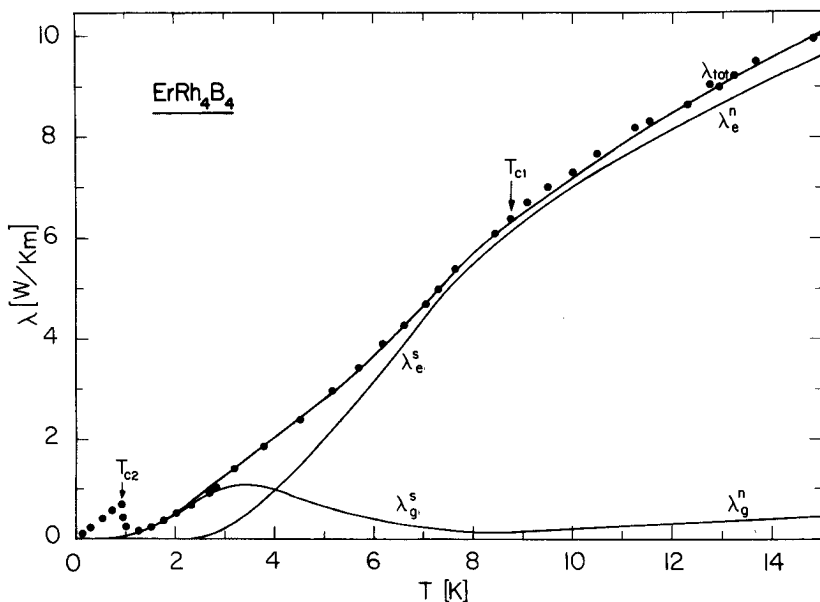
Figure 4.15

Thermal conductivity of $ErRh_4B_4$. Solid lines are the lattice λ_g and electronic λ_e contributions, calculated on the base of the BRT theory, inclucing a boundary scattering term (Odoni, Keller, Ott, Hamaker,Johnston and Maple 1981).

points out that although the pairbreaking effect of the magnetic impurities may be very small in the paramagnetic state it may become very large in the magnetically ordered phase and thus lead to a decrease of the numbers of superconducting electrons or to a quenching of superconductivity.

From the increase of the thermal conductivity in this temperature range we can estimate the order parameter $W(T) = 1 - n_n(T)/n_o$ within the framework of the two fluid model (Gorter and Casimir 1934). n_n is the number

of normal electrons in the superconducting state at a temperature T and n_o the total number of conduction electrons. From figure 4.15 we see that the calculated electronic conductivity at 1.2 K is negligible. To calculate the ratio $n_n(T)/n_o$ we assumed that the increase of the thermal conductivity between 1.2 K and 0.87 K is totally due to the creation of normal electrons and therefore this ratio is given by the ratio of the electronic thermal conductivity in the normal state λ_e^n, given by $\lambda_e^n = 0.76$ Watt/(mK^2), to that in the superconducting state $\lambda_e^s = \lambda_{exp} - \lambda_g$. As a rough estimate we assume that the lattice thermal conductivity at 1.2 K decreases linearly to zero at 0.87 K , taking into account that the occurrence of normal electrons quickly reduces the mean free path of the phonons. Therefore we calculated W(T) by

$$W(T) = 1 - \left\{ 0.76T(W/mK^2)/(\lambda_{exp} - \lambda_g) \right\}^{-1} \qquad (4.10)$$

The calculated behaviour of the order parameter W is shown in figure 4.16 as a function of the temperature. For (4.10) we used the cooling curve of the thermal conductivity.

The two fluid model is a rough description of superconductivity and the consequences have to be considered critically. In reality, magnetic interactions in a superconductor do not only change the number of "normal electrons" but also modify the energy gap and the density of states of the electrons.

The above defined superconducting order parameter W changes over a temperature range of about 0.5 K. We can compare this behaviour with the Bragg intensity of neutron scattering experiments on a similar sample of

- 48 -
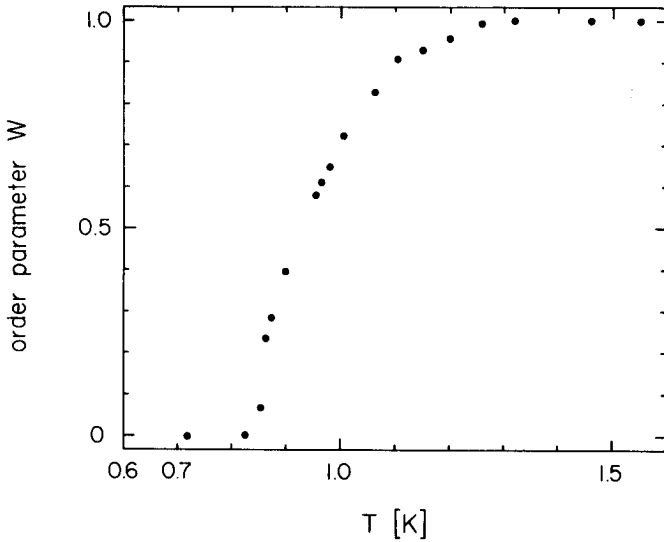
Figure 4.16

Calculated order parameter in the two fluid model of Gorter and Casimir.
The order parameter W(T) is defined in the text.

$ErRh_4B_4$ by Moncton et al (1980). At 0.97 K the superconducting order para-
meter W is 0.6 whereas the normalized magnetisation M/M_o is $\sim$ 0.66. At this
temperature magnetic order exists although 40% of the electrons are still
in the superconducting state.

There are various theoretical attemps to explain the peculiar magnetic
and superconducting properties in this temperature range. Blount and Varma
1979) found in their model that with decreasing temperature the superconduc-
ting state can transform over a narrow temperature range by a second order
transition into a coexistent state of superconductivity with a spiral
structure magnetisation followed by a first order transition to a uniform

magnetic state. Matsumoto, Umezawa and Tachiki (1979) and Bulaevski

Rusinov and Kulić (1979,1980) come to similar conclusions in their model.

In the light of these models, one can interpret the experimental facts.

The thermal hysteresis in resistance, ac magnetic susceptibility, thermal

conductivity and neutron diffraction and the lambda-type anomaly in the

specific heat around 0.9 K indicate a first order transition from a super-

conducting to a normal ferromagnetically ordered state. Small-angle

neutron scattering results near T_{c2} indicate an oscillatory magnetisation

with a wavelength of $\sim$ 100 Å (Moncton et al 1980). Above $\sim$ 1.1 K the small

angle scattering peak disappears and the thermal conductivity shows bulk

superconductivity.

4.5 POSSIBLE COEXISTENCE OF SUPERCONDUCTIVITY AND MAGNETIC ORDER:$SmRh_4B_4$

In the foregoing sections we discussed how the thermal conductivity is affected when a material orders ferromagnetically ($HoRh_4B_4$), when it becomes superconducting ($LuRh_4B_4$) or when it loses its superconductivity upon magnetic ordering as the temperature is decreased ($ErRh_4B_4$). In this section we discuss the case where a substance becomes superconducting and where superconductivity persists below the magnetic ordering temperature.

Previous work (McCallum,Johnston, Maple and Shelton 1977, Ishikawa and Fischer 1977, Azevedo, Clark, Murayama, McCallum, Johnston, Maple and Shelton 1978, Moncton, Shirane, Thomlinson, Ishikawa and Fischer 1978) on rare earth Chevrel-phase compounds has shown that superconductivity may coexist with magnetic order if the magnetic order is antiferromagnetic in nature. Similar behaviour has recently been found in $NdRh_4B_4$ (Hamaker, Woolf, MacKay,Fisk and Maple 1979) and in $SmRh_4B_4$ (Hamaker, Woolf, MacKay, Fisk and Maple 1979, Ott, Odoni, Hamaker and Maple 1980). Both these boride compounds exhibit pronounced anomalies in specific heat and upper critical field, indicating the occurrence of magnetic ordering without destruction of superconductivity.

Reliable confirmation of the persistence of bulk superconductivity with magnetic ordering may be obtained from measurements of the thermal conductivity λ. Therefore we have measured the thermal conductivity of $SmRh_4B_4$ between 0.05 K and 4 K in zero external magnetic field and in external fields up to a value exceeding the critical field. The sample was a parallelepiped of polycrystalline material with dimensions 5.5x1.1x1 mm^3.

In addition we measured the electrical resitivity ρ on this specimen in
the same temperature and magnetic field range. The residual resistance
ratio of this sample is 22.3, the resistivity just above T_c is $3.4 \times 10^{-6} \Omega m$.
The resistively determined critical temperature T_c of our sample is 2.68 K.

In figure 4.17 we show the temperature dependence of the electrical
resistance of $SmRh_4B_4$ in zero magnetic field and in a supercritical magne-
tic field. In zero magnetic field the sample remains superconducting down
to 100 mK. In a field of 2 kOe the sample remains normal down to the same
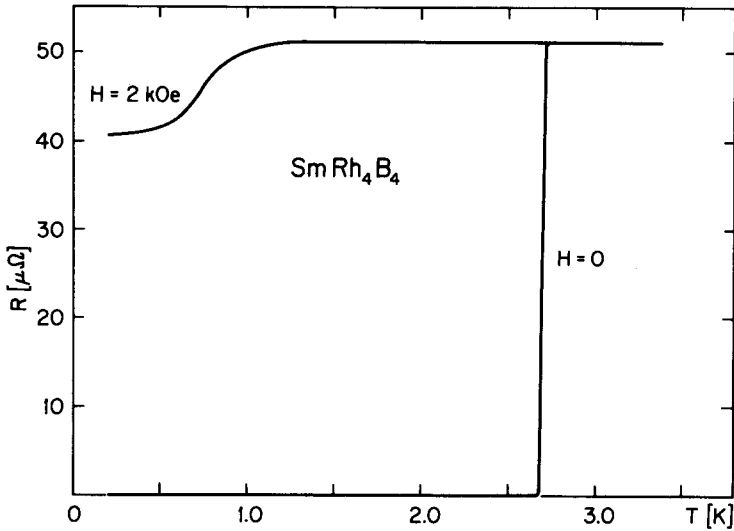temperature. The resistance data of $SmRh_4B_4$ in the normal state are simi-

Figure 4.17
Electrical resistance of $SmRh_4B_4$ for magnetic field H = 0 and H = 2 kOe
(Ott, Odoni, Hamaker and Maple 1980).

lar to those found in $HoRh_4B_4$ where the drop of the resistance is associated with magnetic ordering. Together with the thermal conductivity data (see below) these results confirm the conclusions obtained by Hamaker et al (1979) who suggested that the drop below 1 K may be due to a magnetic phase transition.

In contrast to $ErRh_4B_4$, where the residual resistance above T_{c1} and below T_{c2} differs about 5%, the resistance drop in $SmRh_4B_4$ amounts to 20%. This is an indication of a strong interaction of the conduction electrons with the localized magnetic moments.

Figure 4.18 shows the temperature dependence of the thermal conductivity λ of $SmRh_4B_4$ in zero magnetic field and in a field of 2 kOe. In zero magnetic field and above T_c we find a linear temperature dependence for λ. Below T_c the thermal conductivity falls below the linear temperature dependence. No marked anomaly is found around 0.87 K where the specific heat shows a lambda-type anomaly. Below this magnetic ordering temperature (probably antiferromagnetic, according to the work of Hamaker et al(1979)), λ continues to decrease with decreasing temperature, contrary to the steep rise back to the normal state thermal conductivity observed in $ErRh_4B_4$ as mentioned before. However, the temperature dependence of λ below T_c is not that of an ordinary superconductor. The reduction below the linear temperature dependence at the lowest temperatures is much less than what one would expect from the Bardeen-Rickayzen-Tewordt theory (see also figure 4.18). In a field of 2 kOe, $SmRh_4B_4$ remains normal. The thermal conductivity λ can be divided into two distinct temperature regions with linear temperature dependence. Above $\sim$ 0.9 K λ can be written as $\lambda = 0.95T$ W/K^2m; below about 0.7 K $\lambda = 1.15T$ W/K^2m. The increase of λ and the con-
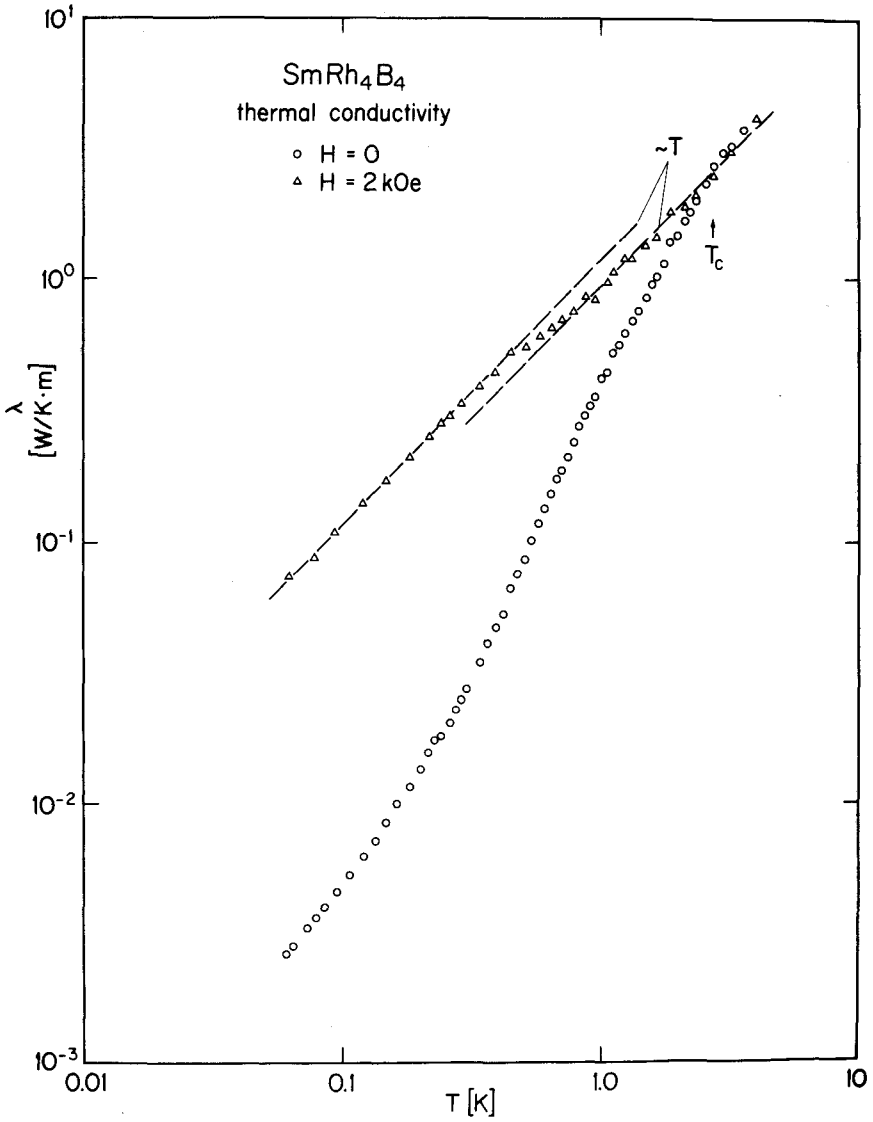
Figure 4.18

Thermal conductivity of $SmRh_4B_4$ between 0.05 K and 4 K for magnetic field
H = 0 and H = 2 kOe (Ott, Odoni, Hamaker and Maple 1980).

comitant drop in ρ on the same sample indicate that one is not dealing with spurious superconducting phases but with a magnetic phase transition instead (Ott et al 1980). The difference in the coefficients of the linear thermal conductivity in the normal state is about 20% and corresponds in magnitude to the drop in the electrical resistance.

The magnetic moments have a strong influence on the electrical resistivity and the thermal conductivity in the normal state and we expect that they influence the thermal conductivity in the superconducting state as well. This situation is discussed in the theory of Ambegaokar and Griffin (1964) (AG theory). The AG theory is based on the Abrikosov-Gor'kov theory on the depression of T_c due to magnetic interactions between localized magnetic moments and conduction electrons and gives the ratio of the electronic thermal conductivity in the superconducting state λ_e^s to that in the normal state λ_e^n. The AG theory has the same limitations as the Abrikosov-Gor'kov theory in that it neglects the correlation between the impurity spins and assumes a random distribution of the magnetic impurities. Below the magnetic ordering temperature the assumption of noninteracting magnetic moments is no more fullfilled and we expect a deviation from the theoretical predictions. On the other hand we assume that the regular distribution of the magnetic moments is no obstacle to the applicability of the AG theory.

The ratio of the electronic thermal conductivities in the superconducting state λ_e^s and in the normal state λ_e^n is given in the AG theory by

$$\lambda_e^s / \lambda_e^n = \frac{3}{2\pi^2} \gamma^3 \int_0^\infty E^2 \mathrm{sech}^2 (V2\gamma E) \, h(E/\Delta, \alpha) dE \tag{4.11}$$

where $\gamma = (k_B T)^{-1}$, E is the excitation energy measured from the Fermi energy and $\Delta(T)$ the Abrikosov-Gor'kov order parameter. The pair breaking

parameter α is defined by

$$\alpha = \frac{n_i/n_{cri}}{2\Delta(T)/\Delta_o(0)} \, . \tag{4.12}$$

$\Delta_o(0)$ is the order parameter at $T = 0$ for the pure superconductor without magnetic impurities. $h(E/\Delta,\alpha)$ is a function defined by

$$h(E/\Delta,\alpha) = V2\left\{1 + \frac{|u^2| - 1}{|u^2 - 1|}\right\} \tag{4.13}$$

where u is given by the equation

$$E/\Delta = u\left\{1 - \frac{i\alpha}{\{u^2 - 1\}^{V2}}\right\}. \tag{4.14}$$

We[1] evaluated (4.11), (4.13), and (4.14) nummerically for different ratios n_i/n_{cri}. The ratio $\Delta(T,n_i/n_{cri})/\Delta_o(0)$ was taken from figure 4 of the paper of Ambegaokar and Griffin (1964). In absence of magnetic impurities, the ratio $\Delta(T)/\Delta_o(0)$ reduces to the BCS relation of the temperature dependence of the energy gap. In this case $h(E/\Delta, \alpha = 0)$ is zero for $E < \Delta(T)$. Therefore (4.11) reduces to the BRT curve for λ_e^s/λ_e^n.

Figure 4.19 shows the calculated ratio (4.11) using a value n_i/n_{cri} of 0.85 together with the experimental results of λ^s/λ^n. Here we assumed that the thermal conductivity in the normal and superconducting state is totally due to electrons. This figure also shows the BRT curve for the pure limit $\alpha = 0$. As one can see, the Ambegaokar-Griffin curve with $n_i/n_{cri} = 0.85$ describes the experimental data above the magnetic ordering temperature T_λ correctly. For lower temperatures the experimental points

---

[1] I thank Dr. W Joss for the calculation of (4.11).
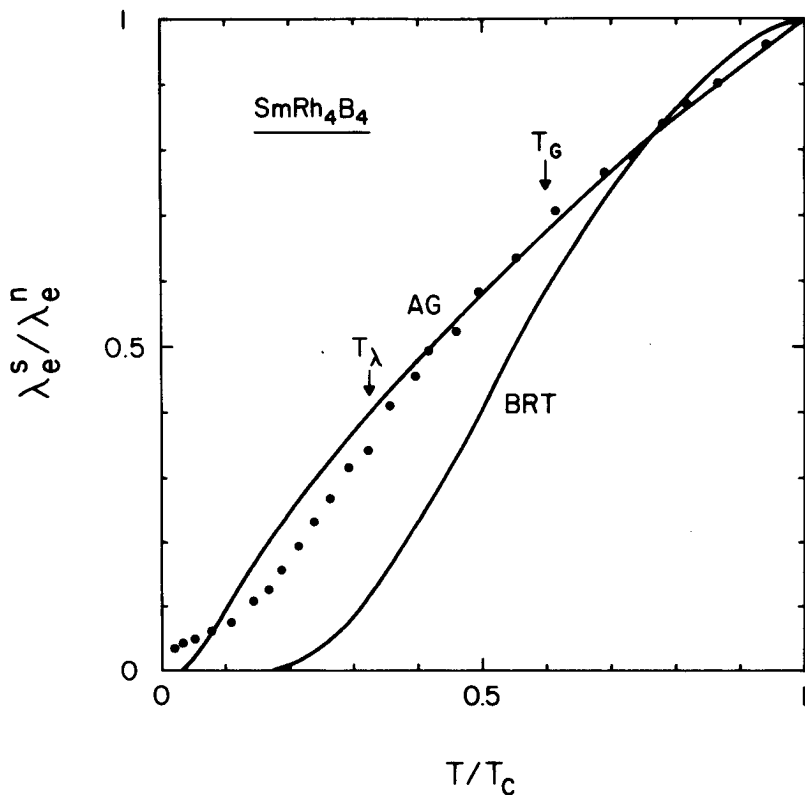
Figure 4.19

Experimental ratio of the electronic thermal conductivity in the supercon-
ducting state to that in the normal state assuming that the thermal con-
ductivity is totally due to the electrons. The solid curves are the theo-
retical predictions of Ambegaokar and Griffin (AG) with $n_i/n_{cri} = 0.85$
and of Bardeen, Rickayzen and Tewordt (BRT). T_λ indicates where a lambda-
type anomaly in the specific heat is found. T_G is described in the text.

the experimental points fall below the theoretical curve of Ambegaokar and Griffin indicating that the assumption of noninteracting magnetic moments is not fullfilled anymore. The decrease below the theoretical curve can be interpreted a a reduction of the pair breaking parameter α and is consistent with H_{c2} measurements of Hamaker (1981) where an additional increase of the critical field H_{c2} below T_λ is found. At the lowest temperatures the ratio of the thermal conductivity in the superconducting state to that in the normal state flattens out, that is, the thermal conductivity in the superconducting state tends to a linear temperature dependence. There are different possibilities to explain this behaviour (Ott et al 1980). A small fraction of normal material extending over the sample length can dominate the thermal conductivity in this low temperature range and therefore lead to a nearly linear temperature dependence. The second possible explanation is the lattice contribution to the thermal conductivity in the superconducting state. In the discussion, we neglected this contribution. This is not justified anymore for the lowest temperatures where the enhancement of the lattice thermal conductivity due to reduced phonon- electron scattering can be appreciable. It also cannot be ruled out that we observe a contribution to the thermal conductivity other than those from electrons and phonons. In the antiferromagnetically ordered state heat may be carried by spin waves (Lüthi 1962). This effect is usually not obseved in metals because of the dominant electronic contribution. However, as far as thermal conductivity is concerned, a superconductor well below its transition temperature can be regarded as an insulator in the sense that only phonons contribute to λ and the spin wave contribution to λ may indeed become observable. The temperature dependence is then given by the dispersion relation of the spins. None of these possibilities can be confirmed with these data.

The effective concentration ratio n_i/n_{cri} found by fitting the experimental λ^s/λ^n to the AG theory is 0.85. There is another way to determine this ratio. An estimate can be gained from the depression of the superconducting critical temperature T_c due to localized magnetic moments compared to the nonmagnetic $LuRh_4B_4$ using the above mentioned Abrikosov-Gor'kov theory. A depression of 3.5 K must be attributed to the nonmagnetic effects by replacing Lu^{3+} ions by Sm^{3+} ions if we assume the validity of a linear interpolation of T_{co} between the $LuRh_4B_4$ and $Lu_{1-x}La_xRh_4B_4|_{x\to1}$ (c.f. figure 4.13). (The compound $LaRh_4B_4$ does not exist). A"nonmagnetic" $SmRh_4B_4$ therefore would have a T_{co} of 8.95 K. The actual critical temperature T_c of $SmRh_4B_4$ is 2.68 K. The estimated ratio T_c/T_{co} is 0.3 which, according to the theory of Abrikosov and Gor'kov on the depression of T_c due to magnetic interactions between localized magnetic moments and conduction electrons, corresponds to a normalized impurity concentration of n_i/n_{cri} = 0.85 in agreement with our value from the thermal conductivity. Hamaker (1981) interpreted the temperature dependence of the critical field H_{c2} in the framework of a theory by Machida which extends the Abrikosov-Gor'kov theory to correlated spin systems. In fitting this theory to the H_{c2} data, Hamaker obtains T_c/T_{co} = 0.55.

In the Abrikosov-Gor'kov theory, a depression of T_c by magnetic impurities is accompanied by a change in the excitation spectrum of the superconductor and always leads to a temperature region below T_c where gapless superconductivity occurs. The extent of this temperature range is given by the condition $\alpha = 1$. In the case of T_c/T_{co} = 0.3 the creation of a gap takes place below T/T_{co} = 0.2. This temperature is marked by the arrow labelled with T_G. For the direct observation of the predicted

gapless region we have to perform tunneling experiments on $SmRh_4B_4$ around and below 1 K.

5 CONCLUSIONS

The variety of magnetic and superconducting properties in the system of rare earth rhodium borides are also reflected in the electrical and the thermal conductivity. The measurements of these transport properties therefore provided valuable information on superconductivity and magnetism.

To study the influence of superconductivity on a compound of this system, we have measured the electrical resistivity and the thermal conductivity of $LuRh_4B_4$ where superconductivity is not influenced by a magnetic phase transition. The detailed analysis of these data showed that the lattice contribute about one third of the total thermal conductivity at the superconducting critical temperature T_c. The electronic thermal conductivity in the superconducting state could be described with the theory of Bardeen, Rickayzen and Tewordt (1958) (BRT). For the lattice thermal conductivity in the superconducting state, we had to include, besides the phonon-electron scattering, a phonon-impurity and a phonon-boundary term. From a fit to our data, the ratio of the energy gap to the superconducting critical temperature was found to be that of a weak coupling superconductor: $2\Delta(0)/k_B T_c = 3.5$.

The compound $HoRh_4B_4$ was chosen to study ferromagnetic order without interference of superconductivity. The behaviour of the thermal conductivity and the electrical resistivity was discussed only qualitatively. The increase in the electrical conductivity and the concomitant enhancement of the thermal conductivity could be interpreted as a mean free path effect of the conduction electrons. The magnetic ordering enhances the mean free path of the electrons due to the reduced spin disorder scattering in the ferromagnetic phase.

The reentrant superconductor $ErRh_4B_4$ shows both phenomena. Between 8.7 K and 1.2 K the compound was found to exhibit superconductivity. We successfully applied the BRT theory of thermal conductivity in this temperature range. Here, the influence of the localized noninteracting magnetic Er^{3+} ions was found to be small. Below 1.2 K we found a gradual increase of the thermal conductivity over a temperature range of about 0.5 K, simultaneously with the onset of magnetic order. Below 0.87 K, the thermal conductivity displayed a linear temperature dependence indicating that the whole sample is in the normal state. The thermal hysteresis found in other physical properties was confirmed by the thermal conductivity measurements.

In $SmRh_4B_4$ the thermal conductivity data showed convincingly that superconductivity remains a bulk property below the magnetic ordering temperature T_λ. In contrast to $ErRh_4B_4$, the localized magnetic moments of Sm^{3+} ions seem to have a strong influence on the thermal conductivity of the superconducting state. We were able to interpret our results in terms of the theory of Ambegaokar and Griffin (1964) on thermal conductivity in a superconductor containing magnetic impurities. From a fit to our data we derived a pair-breaking parameter which is consistent with an estimated value deduced from the reduction of the superconducting critical temperature due to magnetic interactions.

6 SUMMARY

We have measured the thermal conductivity and the electrical resistivity of
$LuRh_4B_4$, $HoRh_4B_4$, $ErRh_4B_4$ and $SmRh_4B_4$ between 0.05 K and 50 K. The properties
of these four compounds are characteristic for the whole series of the
rare earth rhodium borides.

$LuRh_4B_4$ shows superconductivity. A detailed analysis shows that the
lattice contributes about one third of the total thermal conductivity at
the critical temperature T_c. The thermal conductivity in the superconduc-
ting state can be described with the theory of Bardeen, Rickayzen and
Tewordt (BRT). From a fit to our data, the ratio of the energy gap to the
superconducting critical temperature is found to be that of a weak coupling
superconductor: $2\Delta(0)/k_BT_c = 3.5$.

$HoRh_4B_4$ orders ferromagnetically. The behaviour of the thermal conduc-
tivity and the electrical resistivity below the ordering temperature can
be explained in terms of an enhanced mean free path due to the decrease of
spin disorder scattering in the ferromagnetic phase.

The reentrant superconductor $ErRh_4B_4$ shows superconductivity and ferro-
magnetic order. The effect of the noninteracting localized magnetic moments
of the Er^{3+} ions on the superconductivity is weak and the BRT theory may be
applied. The thermal conductivity data show a gradual destruction of super-
conductivity over a temperature range of 0.5 K with the onset of magnetic
order. Below 0.87 K, the thermal conductivity displays a linear temperature
dependence indicating that the whole sample is in the normal state. The ther-
mal hysteresis around 0.9 K found in other physical properties was confirmed

by the thermal conductivity measurements.

Superconductivity and possibly antiferromagnetic ordering persists in $SmRh_4B_4$. In contrast to $ErRh_4B_4$, the localized magnetic moments of Sm^{3+} ions seem to have a strong influence on the thermal conductivity in the superconducting state. Our results can be interpreted in terms of the Ambegaokar and Griffin theory of the thermal conductivity in a superconductor containing magnetic impurities. In particular we derive a pairbreaking parameter which is consistent with the value deduced from the reduction of the superconducting critical temperature due to magnetic interactions. From the value of this parameter and following the Abrikosov and Gor'kov theory of magnetic impurities in superconductors we expect a gapless super-conducting region for $T/T_c > 0.65$.

REFERENCES

Abrikosov, A.A. and Gor'kov, L. P. 1960 Zh. Exsp. Theor. Fiz. $\underline{39}$, 1781-1796.

    (Sov. Phys. JETP $\underline{12}$, 1243-1253)

Ambegaokar, V. and Griffin, A. 1964 Phys. Rev. $\underline{A4}$, 1151-1167.

Anderson, A. C. Salinger, G. L. and Wheatley, J. C. 1961 Rev. Sci. Instrum.

    $\underline{32}$, 1110-1112.

Azevedo, L. J. Clark, W. G. Murayama, C. McCallum, R. W. Johnston, D. C.

    Maple, M. B. and Shelton, R. N. 1978 J. Phys. Suppl. $\underline{C6}$, 365-366.

Bardeen, J. Cooper, L. N. and Schrieffer, J. R. 1957 Phys. Rev. $\underline{108}$, 1175-1204.

Bardeen, J. Rickayzen, G. and Tewordt, L. 1958 Phys. Rev. $\underline{113}$, 982-994.

Bass, J. 1972 Advances in Physics $\underline{21}$, 431-604.

Berman, R. 1976 Thermal Conduction in Solids, Oxford: Claredon Press.

Blount, E. I. and Varma, C. M. 1979 Phys. Rev. Lett. $\underline{16}$, 1079-1082.

Bobetic, V. M. 1964 Phys. Rev. $\underline{A136}$, 1535-1538.

Bulaevski, L. N. Rusinov, A. I. and Kulic, M 1979 Solid State Commun.

    $\underline{31}$, 59-63.

Bulaevski, L. N. Rusinov, A. I. and Kulic, M. 1980 J. Low temp. Phys.

    $\underline{39}$, 255-272.

Clement, J. R. and Quinell, E. M. 1952 Rev. Sci. Instr. $\underline{23}$, 213-216.

Fertig, W. A. Johnston, D. C. DeLong, L. E. McCallum, R. W. Maple, M. B.

    and Matthias, B. T. 1977 Phys.Rev. Lett. $\underline{38}$, 987-990.

Fischer, $\emptyset$. Ishikawa, M. Pelizzone, M. and Treyvaud, A. 1979 J. Phys.

    Colloq. $\underline{40}$, C5-89, 89-94.

Geilikman, B. T. 1958 Zh. Exsp. Theor. Fiz. $\underline{34}$, 1042-1044. (Sov. Phys.

    JETP $\underline{7}$, 721-722)

Geilikman, B. T. and Kresin, V. Z. 1958 Sov. Phys. Dokl. $\underline{3}$, 1161-1163.

Ginsburg, V. L. 1956 Zh. Exsp. Theor. Fiz. $\underline{31}$, 202-210. (Sov. Phys. JETP $\underline{18}$, 153-160)

Gorter, C. J. and Casimir, H. B. G. 1934 Physica $\underline{1}$, 306-320.

Gupta, A. K. and Wolf, S. 1972 Phys. Rev. $\underline{B6}$, 2595-2602.

Hamaker, H. C. Woolf, L. D. MacKay, H. B. Fisk, Z. and Maple, M. B. 1979 Solid State Commun. $\underline{31}$, 139-144.

Hamaker, H. C. Woolf, L. D. MacKay, H. B. Fisk, Z. and Maple, M. B. 1979 Solid State Commun. $\underline{32}$, 289-294.

Hamaker, H. C. 1981 Doctoral dissertation, University of California, San Diego.

Harris, F. K. 1934 J. Natl. Bur. Stand. $\underline{13}$, 391-411.

Hein, R.A. Falge, Jr. Matthias, B. T. and Corenzwit, C. 1979 Phys. Rev. Lett. $\underline{42}$, 500-502.

Ishikawa, M. and Fischer, $\emptyset$. 1977 Solid State Commun. $\underline{24}$, 747-751.

Kadanoff, P. L. and Martin, P. C. 1961 Phys. Rev. 124, 670-697.

Kittel, C. 1971 Introduction to Solid State Physics, 4th ed. New York: John Wiley&Sons.

Klemens, P. G. 1951 Proc. R. Soc. $\underline{A208}$, 108-133.

Klemens, P. G. 1956 In: Handbuch der Physik, vol 14, pp 198-276, Berlin, Göttingen, Heidelberg: Springer.

Klemens, P. G. and Tewordt, L. 1964 Rev. Mod. Phys. $\underline{36}$, 118-120.

Lindenfeld, P. and Rohrer, H. 1965 Phys.Rev. $\underline{139}$, 206-211.

Lounasmaa, O. V. 1974 Experimental Principles and Methods Below 1 K, London: Academic Press.

Lüthy, B. 1962 J. Phys. Chem. Solids $\underline{23}$, 35-38.

MacKay, H. B. 1979 Doctoral dissertation, University of California, San Diego.

MacKay, H. B. Woolf, L. D. Maple, M. B. and Johnston, D. C. 1980
  1980 J. Low Temp. Phys. 41, 639-651.

Matthias, B. T. Corenzwit, J. E. Vandenberg, J. M. and Barz, H. 1977
  Proc. Natl.Acad. Sci. 74, 1334-1335.

Matthiessen, A. 1864 Ann. Physik 122, 19.

Maple, M. B. Hamaker, H. C. Johnston, D. C. MacKay, H. B. and Woolf, L. D.
  1978 J. Less Common Metals 62, 251-263.

Matsumoto, H. Umezawa, H. and Tachiki, M. 1979 Solid State Commun. 31,
  157-161.

McCallum, R.W. Johnston, D. C. Shelton, R. N. Fertig, W. A. and Maple,
  M. B. 1977 Solid State Commun. 24, 501-505.

Moncton, D. E. McWhan, D. B. Eckert, J. Shirane, G. and Thomlinson, W.
  1977 Phys. Rev. Lett. 39, 1164-1166.

Moncton, D. E. Shirane, G. Thomlinson, W. Ishikawa, M. and Fischer, Ø.
  1978 Phys. Rev. Lett. 41, 1133-1136.

Moncton, D. E. McWhan, D.B. Schmidt, P. H. Shirane, G. Thomlinson, W.
  Maple, M. B. MacKay, H. B. Woolf, L. D. Fisk, Z. and Johnston, D.C.
  1980 Phys. Rev. Lett. 45, 2060-2063.

Mühlschlegel, B. 1959 Z. Phys. 155, 313-327.

Odoni, W. and Ott, H. R. 1979 Phys. Lett. A70, 480-483.

Odoni, W. Keller, G. Ott, H. R. Hamaker, H. C. Johnston, D. C. and Maple,
  M. B. 1981 Proc. Int. Conf. on Low Temp. Phys. 16, (Los Angeles),
  to be published.

Ott, H. R. Fertig, W. A. Johnston, D. C. Maple, M. B. and Matthias, B. T.
  1978 J. Low Temp. 33, 159-174.

Ott, H. R. Odoni, W. Hamaker, H. C. and Maple, M. B. 1980 Phys. Lett.
  A75, 243-245.

Ott, H. R. and Odoni, W. 1980 In Superconductivity in d - and f - Band Metals, pp403-408, New York: Academic Press.

Ott, H. R. Woolf, L. D. Maple, M. B. and Johnston, D. C. 1980 J. Low Temp. Phys. 39, 383-395.

Ott, H. R. Keller, G. Odoni, W. Woolf, L. D. Maple, M. B. Johnston, D. C. and Mook, H. A. to be published.

Ott. H. R. Campbell, A. M. Rudigier, H. Hamaker, H. C. and Maple, M. B. 1981 Proc. Int. Conf. on Low Temp. Phys. 16 (Los Angeles), to be published.

Olsen, J. L. 1952 Proc. Phys. Soc. A65, 518-532.

Olsen, J. L. and Rosenberg, H. M. 1953 Philos. Mag. Suppl. 2, 28-66.

Ramos, E. D. and Sanchez, D. H. 1974 Cryogenics 14, 341-343.

Rhodes, P. 1951 Proc. R. Soc. A204, 396-405.

Roth, S. 1978 Appl Phys. 15, 1-11.

Schneider, S. C. Levy, M. Johnston, D.C. and Matthias B. T. 1980 Phys. Rev. Lett. A80, 72-74.

Sousa, J. B. 1969 J. Phys. C2, 629-639.

Taylor, K. N. R. and Darby, M. I. 1972 Physics of Rare Earth Solids, London: Chapman and Hall LTD.

Vandenberg, J. M. and Matthias, B. T. 1977 Proc. Natl. Acad. Sci. 74, 1336-1337.

Wheatley, J. C. Vilches, O. E. and Able, W. R. 1968 Physics 4, 1-64.

Wheatley, J. C. Rapp, R. E. and Johnson, R. E. 1971 J. Low Temp. Phys. 4, 1-39.

Woolf, L. D. Johnston, D. C. MacKay, H. B. McCallum, R. W. and Maple, M. B. 1979 J. Low Temp. Phys. 35, 651-669.

Woolf, L. D. 1980 Doctoral dissertation, University of Calif., San Diego.

Wyder, P. 1965 Phys. Kondens, Materie $\underline{3}$, 292-302.

Ziman, J. M. 1960 Electrons and Phonons, Oxford: Claredon Press.

ZUSAMMENFASSUNG

Wir haben thermische und elektrische Leitfähigkeiten von $LuRh_4B_4$, $HoRh_4B_4$, $ErRh_4B_4$ und $SmRh_4B_4$ im Temperaturbereich von 0.05 K bis 50 K gemessen. Diese vier Verbindungen charakterisieren die magnetischen und supraleitenden Eigenschaften des ganzen Systems der Seltenen Erd Rhodium Boride.

$LuRh_4B_4$ ist ein Supraleiter. Eine detailierte Analyse zeigt, dass an der kritischen Temperatur der Supraleitung ein Drittel der gesamten Wärmeleitung von den Phononen herrührt. Die Wärmeleitung im supraleitenden Zustand kann mit der Theorie von Bardeen, Rickayzen und Tewordt (BRT) beschrieben werden. Aus einem Fit auf unsere Wärmeleitungsdaten wurde das Verhältnis der Energielücke bei T = 0 zur kritischen Temperatur T_c bestimmt. Danach ist dieses Verhältnis das eines schwach koppelnden Supraleiters: $2\Delta(0)/k_bT_c = 3.5$.

$HoRh_4B_4$ ordnet ferromagnetisch. Das Verhalten der thermischen Leitfähigkeit und des elektrischen Widerstandes kann auf einen Freie Weglängeneffekt zurückgeführt werden. Durch das Wegfallen der Spinunordnungsstreuung vergrössert sich die Freie Weglänge der Elektronen.

$ErRh_4B_4$ zeigt Supraleitung und Ferromagnetismus. Da der Einfluss der nichtkoppelnden lokalisierten magnetischen Momente der Er^{3+} Ionen schwach ist, kann man die BRT Theorie anwenden. Die Wärmeleitung zeigt, dass mit dem Einsetzen der langreichweitigen magnetischen Ordnung die Supraleitung langsam zerstört wird. Der Bereich dieses Ueberganges erstreckt sich auf ungefähr 0.5 K. Unterhalb 0.87 K weist die Wärmeleitung eine lineare Temperaturabhängigkeit auf wie wir sie von einem normalen Metall bei tiefen

Temperaturen erwarten. Um 0.9 K zeigt auch die Wärmeleitung eine ther-
mische Hysterese wie sie in anderen physikalischen Eigenschaften gefunden
wurde.

In $SmRh_4B_4$ sind Supraleitung und antiferromagnetische Ordnung gleich-
zeitig vorhanden. Die magnetischen Sm^{3+} Ionen scheinen hier einen viel
stärkeren Einfluss auf die Supraleitung zu haben. Wir analysierten unsere
Resultate im Rahmen einer Theorie von Ambegaokar und Griffin die die Wärme-
leitung eines Supraleiters mit magnetischen Verunreinigungen beschreibt.
Die Uebereinstimmung oberhalb der magnetischen Ordnungstemperatur ist gut.
Im speziellen haben wir einen Paarbrechungsparameter für Cooperpaare abge-
leitet, der mit dem Wert aus einer Abschätzung mit Hilfe der Reduktion
der kritischen Temperatur aufgrund von magnetischen Verunreinigungen über-
einstimmt. Aufgrund des Wertes dieses Parameters erwarten wir einen Tempera-
turbereich $T_c > T/T_c > 0.65$ wo Supraleitung ohne Energielücke auftreten sollte.

- 71 -

Mein Dank

Ich möchte zum Schluss all jenen Danken, die mir diese Arbeit erst

ermöglichten.

In Prof. Dr. J.L. Olsen fand ich in dieser Zeit die ideale Mischung

aus Freiheit und Führung und er gab mir immer wieder neue Einsichten

in die Physik. Dr. H.R. Ott führte mich in das faszinierende Gebiet

der tiefsten Temperaturen ein. Mit Dr. W. Joss, Dr. R. Monnier, Prof.

P. Martinoli und Prof. B.S. Chandrasekhar durfte ich viele klährende

Diskussionen führen. Hans Thomas, Paul Caminada und Albert Vogelsanger

halfen mir in allen technischen Fragen. Den Mitarbeitern aus den

Gruppen von Prof. B.T. Matthias und Prof. M.B. Maple verdanke ich die

Proben für unsere Messungen. Bei meinen Kollegen Benno Barbisch, David

Ernest, Dr. Kurt Kwasnitza, Daniel Marek, Dr. A.C. Mota, Helmut Rudigier,

Dominique Salathé und Jean-Claude Weber möchte ich mich nicht nur für

die vielen fachlichen Diskussionen sondern auch für die vielen Stunden

ausserhalb der Physik bedanken, in denen der nötige Ausgleich ge-

schaffen wurde. Marisa Van der Mark und Frl. Molinari unterstützten

mich in allen administrativen Belangen.

Die Arbeit wurde teilweise vom Schweizerischen Nationalfonds finanziert

wofür ich mich an dieser Stelle bedanken möchte.

Walter Coloni

Lebenslauf

1950   geboren in Luzern

1957 - 1962 Primarschule in Hochdorf

1962 - 1970 Mittelschule im Kollegium St. Fidelis in Stans

1970   Maturität Typus B

1970 - 1975 Studium der Physik an der Eidgenössischen Technischen

                    Hochschule in Zürich

1975   Diplomabschluss mit Diplomarbeit in der Gruppe Prof.

                    Dr. J.L. Olsen über "Einfluss von Chrom- Mangan- und

                    Eisenverunreinigungen auf die kritische Temperatur der

                    A 15 Struktur V_3Ga"

1975 - 1981 Wissenschaftlicher Mitarbeiter und Assistent in der

                    Tieftemperaturgruppe von Prof. Olsen

1981   Doktorarbeit "Influence of Superconductivity and Magnetism

                    on Transport Properties of Rare Earth Rhodium Boride

                    Compounds"

Seit 1981   Anstellung im Rahmen eines Projekts des Schweizerischen

                    Nationalfonds an der ETH